



Magnitude and source area estimations of severe prehistoric earthquakes in the western Eastern Alps

Patrick Oswald¹, Michael Strasser¹, Jens Skapski², Jasper Moernaut¹

5 ¹Department of Geology, University of Innsbruck, Innsbruck, 6020, Austria

²Risklayer GmbH, Karlsruhe, 76131, Germany

Correspondence to: Patrick Oswald (oswald.patrick@gmx.net)

Abstract

In slowly deforming intraplate tectonic regions such as the Alps only limited knowledge exists on the occurrence of severe earthquakes, their maximum possible magnitude and their potential source areas. This is mainly due to long earthquake recurrence rates exceeding the time span of instrumental earthquake records and historical documentation. Lacustrine paleoseismology aims at retrieving long-term continuous records of seismic shaking. A paleoseismic record from a single lake provides information on events for which seismic shaking exceeded the intensity threshold at the lake site. In addition, when positive and negative evidence for seismic shaking from multiple sites can be gathered for a certain time period, minimum magnitudes and source locations can be estimated for paleo-earthquakes by a reverse application of an empirical intensity prediction equation in a geospatial analysis. Here, we present potential magnitudes and source locations of four paleo-earthquakes in the western Eastern Alps based on the integration of available and updated lake paleoseismic data. The paleoseismic records at Plansee and Achensee covering the last ~10 kyrs were extended towards the age of lake initiation after deglaciation to obtain the longest possible paleoseismic catalogue at each lake site. Our results show that 25 severe earthquakes are recorded in the four lakes Plansee, Piburgersee, Achensee and potentially Starnbergersee over the last ~16 kyrs, from which four earthquakes are interpreted to left imprints in two or more lakes. Earthquake recurrence intervals range from ca. 1,000 to 2,000 years with a weakly periodic to aperiodic recurrence behavior for the individual records. We interpret that relatively shorter recurrence intervals in the more orogen-internal archives Piburgersee and Achensee are related to enhanced tectonic loading, whereas a longer recurrence rate in the more orogen-external archive Plansee might reflect a decreased stress transfer across the current-day enhanced seismicity zone. Plausible epicenters of paleo-earthquake scenarios coincide with the current enhanced seismicity regions. Prehistoric earthquakes with a minimum moment magnitude (M_W) 5.8-6.1 might have occurred around the Inn valley, the Brenner region and the Fernpass-Loisach region, and might have reached up to M_W 6.3 at Achensee. The paleo-earthquake catalogue might hint at a shift of severe earthquake activity near the Inn valley from east to west to east during Postglacial times. Shakemaps highlight that such severe earthquake scenarios not solely impact the enhanced seismicity region of Tyrol, but widely affect adjacent regions like southern Bavaria in Germany.



1 Introduction

35 Lake paleoseismic studies in different tectonic settings have demonstrated that seismic shaking can leave specific traces in lacustrine sedimentary archives e.g. by basin-wide mass wasting or in-situ soft-sediment deformation above a certain intensity threshold at the lake site (Ayşar et al., 2016; Doughty et al., 2014; Howarth et al., 2014; Monecke et al., 2004; Petersen et al., 2014; Praet et al., 2017; Strasser et al., 2013). As glacigenic lakes are often characterized by continuous sedimentation since deglaciation, they can have continuously recorded earthquakes since then. Especially in slowly

40 deforming, intraplate tectonic settings like the Alps, recurrence rate of severe earthquakes often exceed the timespan of historical earthquake documentation (Beck, 2009; Brooks, 2018; Kremer et al., 2017; Moernaut, 2020; Simonneau et al., 2013). Therefore, long-term lake paleoseismic records provide valuable data to better constrain the recurrence rate and the maximum possible magnitude of severe earthquakes. However, the epicenter location, magnitude and rupture extent of the event mostly remains unknown solely based on a lacustrine paleoseismic archive. Moreover, on-fault evidence are hardly

45 preserved in the Alps due to penetrative anthropogenic landscape modification, gravitational slope processes and relatively high erosion rates (Ustaszewski and Pfiffner, 2008). The so far unraveled active faults are only discovered in special environments, such as displaced Roman archeological remains (Galadini and Galli, 1999), tectonically damaged speleothems (Plan et al., 2010) and in the sedimentary infills of lakes (Fabbri et al., 2017, 2021; Gasperini et al., 2020; de La Taille et al., 2015; Oswald et al., 2021a). To date, two different ground motion modelling methods have been developed to overcome

50 these problems. The first method calculates potential magnitude-epicenter assemblages over a grid based on positive/negative shaking evidence of a certain intensity threshold using a backward application of an intensity prediction equation (IPE; Strasser *et al.*, 2006; Kremer *et al.*, 2017 after Bakun & Wentworth, 1997). The second method calculates potential source faults, the rupture length and the magnitude in a forward modelling approach, which equally handles positive/negative shaking evidence and considers the uncertainty of the IPE (Vanneste et al., 2018). However, this method

55 requires an accurate map of potentially active faults, which is complicated in the Alps due to the vast amount of faults within a confined space for which only limited knowledge exists on their subsurface continuation and interrelation to other faults. Recent lacustrine paleoseismological studies in the western Eastern Alps retrieved three continuous paleoseismic archives covering the Holocene (Oswald et al., 2021a, 2021b). This study aims to extend these existing paleoseismic records in the western Eastern Alps towards the timing of lake initiation where applicable. We compare the timing and relative imprint size

60 of earthquake-related deposits. Based on this we evaluate potential single earthquake events with multiple lake imprints and calculate recurrence statistics on the paleo-earthquake catalogue of the region. Furthermore, we provide possible earthquake parameters of paleo-earthquakes that can explain the observational sedimentological evidence in the lakes and discuss our results in the context of seismicity in intraplate tectonic settings.



65 2 Setting

The study area is located within the western Eastern Alps mainly composed of Austroalpine basement units in the south of the thin-skinned nappe stack of the Northern Calcareous Alps (Fig. 1). Towards the north, the Northern Calcareous Alps superimpose the Helvetic units, the Rhenodanubian flysch and the Alpine foreland molasse. Penninic and subpenninic units outcrop in the Tauern window and the Engadin window in the southeastern and the southwestern study area, respectively.

70 The tectonic units are divided by deep-reaching crustal faults e.g. the Inntal shear zone, Fernpass-Loisach fault system or the

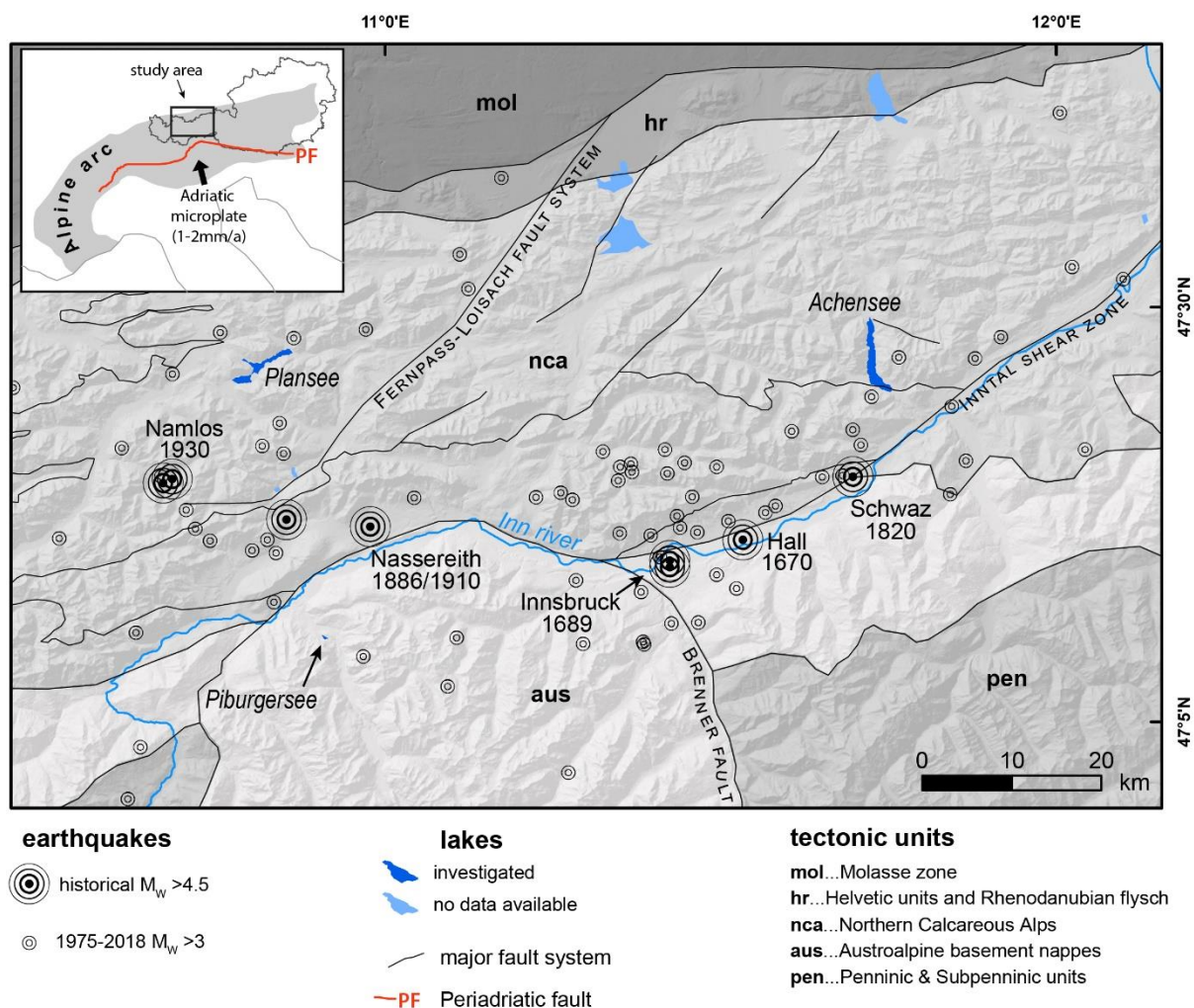


Figure 1 Overview map of the study area. The investigated lakes are located within the Northern Calcareous Alps and Austroalpine basement units subdivided and dissected by large-scale fault systems. Recent seismicity is concentrated in a 100 km wide E-W oriented zone around the Inn valley and along the Fernpass-Loisach fault system. Severe historical earthquakes are also documented in these regions. Earthquake data derived from Stucchi et al. (2013) and Reiter et al. (2018). Inlet shows N-ward indentation of the Adriatic microplate into the Eastern Alps delimited by the Periadriatic fault (PF).



Brenner fault (Eisbacher and Brandner, 1996; Mancktelow et al., 2015; Ortner et al., 2006). These faults were mainly active together with the Periadriatic fault south of the study area in Cenozoic times caused by NNW-ward indentation of the Adriatic microplate in the south and slab-rollback in the eastern Pannonian basin leading to lateral escape tectonics (Ratschbacher et al., 1991; Rosenberg et al., 2004). GPS measurements show that the Adriatic microplate is still pushing northward with about 1-2 mm/a (Métois et al., 2015) causing moderate seismicity with dominant N-S thrust faulting mechanisms focused in a 100 km wide E-W zone in the Inn valley (Fig. 1; Reiter *et al.*, 2018). This zone of enhanced seismicity also hosted a few severe historically documented earthquakes (Hammerl, 2017; Hammerl et al., 2012; Stucchi et al., 2013). Recent studies established three paleoseismic records in the study area spanning the last 10 kyrs by hydroacoustic imaging of the lake subsurface and sediment core analyses in the lakes Plansee, Piburgersee and Achensee (Fig. 1; Oswald *et al.*, 2021a; b). Earthquake imprints are expressed as seismic-stratigraphic horizons of multiple, coeval mass-transport deposits (MTDs) directly overlain by a (mega-)turbidite in seismic data of Achensee and Plansee, whereas in Piburgersee seismic shaking caused in-situ soft-sediment deformation structures (SSDS).

3 Methods

3.1 Extension of the paleoseismic records and event-scaling

The paleoseismic records of Plansee and Achensee are extended further back in time by i) the investigation of outstanding turbidite deposits within the glaciolacustrine sediments by visual analyses of X-ray computer tomographic (CT) and core image data in deeper core sections (only Plansee), and by ii) extending the age-depth models beyond the reach of the core towards initiation of glaciolacustrine sedimentation interpreted on seismic data, which allows the timing of multiple, coeval MTD horizons to be estimated. The sediment depth between the base of the core and the interpreted horizon of the onset of glaciolacustrine sedimentation is calculated using the two-way travel time (TWT) in seismic data and a mean acoustic velocity of the glaciolacustrine seismic unit (~1610 m/s) derived from p-wave velocity measurements on the 12-15 m subsurface depth interval of the cores that recovered the upper part of the glaciolacustrine unit. For the age-depth modelling, we used the broad age range 15-17 ka BP as input age for the onset of glaciolacustrine sedimentation, based on the age-bracketing of glacier readvancement (~17 ka BP) and their final moraine termination (~15 ka BP; Ivy-Ochs *et al.*, 2008). This results in the extension of the pre-existing age-depth models (Oswald et al., 2021a, 2021b) covering the entire sequence of glaciolacustrine and lacustrine sedimentation from the deglaciation of the basin to the present day. Age-depth models from the long cores Plan18-L1 at Plansee and ACH19-L3 at Achensee (Oswald *et al.*, (2021a; b) are based on a combination of short-lived radionuclides (²¹⁰Pb and ¹³⁷Cs) and radiocarbon dates (Table S1) and calculated using the R-package Bacon version 2.5.0 (Blaauw and Christen, 2011). For the age-depth modelling, event deposits with thickness of >5 cm are deleted to obtain an event-free sediment depth. In order to obtain also an event-free sediment depth for the calculated sediment depth below the reach of the core, we assume a constant sedimentation rate and comparable amount and thickness of event deposits as in the cored section of glaciolacustrine sediments.



In principle, an earthquake causes a specific sedimentary imprint when a certain, lake specific seismic intensity threshold is exceeded (e.g. Monecke *et al.*, 2004; Van Daele *et al.*, 2015). Above this threshold, measurements of the sedimentary
105 imprints such as outstanding turbidite thickness (Moernaut *et al.*, 2014) or the occurrence of postseismic landscape response (Howarth *et al.*, 2016) might actually indicate much higher intensities. Therefore, the inferred earthquake events are relatively scaled above the lake's individual intensity threshold based on their imprint size. For Piburgersee, SSDS are scaled based on three development stages ranging from folded layer, incipient breccia to intraclast breccia with increasing intensity (Molenaar *et al.*, 2021; Oswald *et al.*, 2021b; Wetzler *et al.*, 2010) including the deposit thickness and a normalization to the
110 range 0 to 1. The largest imprint in each record corresponds to a value of 1. At Plansee and Achensee, events are relatively scaled based on the MTD volume (V) and turbidite thickness (T) as follows: In a first step, V is divided by the slope area and T is divided by the ratio of the slope area (A_{slope}) to basin area (A_{basin}) to make the imprints of several lakes with different morphometric characteristics comparable (equations 1 and 2).

$$V_{\text{corr}} = \frac{V}{A_{\text{slope}}} \quad (1)$$

$$115 \quad T_{\text{corr}} = \frac{T}{A_{\text{slope}}/A_{\text{basin}}} \quad (2)$$

V is obtained from mapping MTDs in reflection seismic data, A_{slope} and A_{basin} are derived from spatial analysis of bathymetric data and T is measured from the sediment core. The total MTD volume is strongly dependent on the slope area but does not change with basin area. The turbidite thickness is dependent on both, the slope and the basin area, because e.g. a small depocenter surrounded by large slopes would result in a relatively thicker turbidite. To calculate a scaled sedimentary
120 imprint SED_{scaled} , the morphometrics-corrected MTD volume (V_{corr}) and turbidite thickness (T_{corr}) are normalized to the range 0 to 1, where the largest V_{corr} and T_{corr} corresponds to a value of 1, and summed up. Along the Alpine Fault in New Zealand, postseismic landscape response was documented to indicate 1-2 intensity levels higher than events that lack such response (Howarth *et al.*, 2016), but in our case study there is no quantitative data to confidently determine this value for incorporation in the event scaling. In order to also add the occurrence of postseismic landscape response (L) as this third
125 parameter, we define $L = 1$ for events with postseismic landscape response and $L=0$ for events without landscape response. In a last step, SED_{scaled} of the individual records are normalized to the range of 0 to 1 for a better comparison between different paleoseismic records (equation 3).

$$SED_{\text{scaled}} = \frac{(V_{\text{corr}} i - \min(V_{\text{corr}}))}{(\max(V_{\text{corr}}) - \min(V_{\text{corr}}))} + \frac{(T_{\text{corr}} i - \min(T_{\text{corr}}))}{(\max(T_{\text{corr}}) - \min(T_{\text{corr}}))} (+L) \quad (3)$$

3.2 Recurrence statistics

130 The earthquake recurrence interval (in years) is calculated on the interevent times obtained on each lake record. To account for dating uncertainty, interevent times are derived from all individual age-depth model simulations in the software Bacon resulting in a range of possible recurrence intervals. For records with a relatively long open end (> 1000 years) since the last event, recurrence interval calculation is carried out once only considering the closed interevent times and a second time



where an imminent event in the following year is assumed (cf. Griffin *et al.*, 2020). In this way, we also consider the elapsed
135 time since the last event as minimum value for the latest interevent time. Additionally, insights into the recurrence pattern of
earthquakes (i.e. aperiodicity) of the lake records are obtained from the calculation of burstiness, which is directly
transformed from the coefficient of variation (CoV) representing the mean-normalized standard deviation of the interevent
times (Goh and Barabási, 2008). In analogy to the recurrence interval, burstiness and CoV are calculated on interevent times
140 derived from all age-depth model simulations of each record (Kempf and Moernaut, 2021). We subdivide recurrence
patterns, where a paleoseismic record with burstiness -1 to -0.33 (CoV < 0.5) is strongly periodic, -0.33 to -0.05 (CoV 0.5-
0.9) is weakly periodic, -0.05 to 0.05 (CoV 0.9-1.1) is aperiodic and 0.05 to 1 (CoV > 1.1) is bursty. It has to be noted that
our approach does not incorporate the uncertainty in the estimation of burstiness due to the limited event number, i.e. there is
a tendency to underestimate the burstiness of the true population mean (Kempf and Moernaut, 2021; Williams *et al.*, 2019).
However, we consider this approach appropriate for first order estimations, especially given the fair amount of paleoseismic
145 events (8-11) in each record and the record continuity. In addition, we calculated recurrence interval and burstiness of the
regional event record, where the individual events of all three lakes, each comprising all ages of the individual age-depth
model simulations are sorted by their mean age. This has the advantage that the stratigraphic order is also retained for the
recurrence rate within the individual records, but samples somehow randomly between the different records.
Hence, this sampling technique does not artificially overestimate the recurrence intervals of subsequent events within an
150 individual record, which is the case for a pure random sampling between event ages of several records. However, recurrence
intervals might be slightly underestimated when shifting from one record to another, as the sampling might not be
completely random due to the prior defined event order.

3.3 Source area and magnitude reconstruction of paleo-earthquakes

Reconstruction of potential source areas and magnitudes of paleo-earthquakes is based on a two-step geospatial grid-search
155 analysis (Strasser *et al.*, 2006, 2013; Kremer *et al.*, 2017 after Bakun and Wentworth, 1997) reversely applying the empirical
IPE developed for deep earthquakes in the Swiss Alps which is also applicable for $>M_w$ 5.5 earthquakes (Fäh *et al.*, 2011).
The input parameters consist of the intensity threshold for generating lacustrine mass wasting or soft-sediment deformation
structures (SSDS), along with site coordinates of positive and negative evidence for seismic shaking that exceeds this
threshold. In this study, we consider earthquake-related deposits i.e. enhanced mass wasting or SSDS as potentially coeval
160 for the calculation of paleo-earthquake scenarios when more than 40% of the 95% probability density functions (PDFs) of
the event ages overlap. If a lake recorded earthquake-related deposits at the observed event period, the intensity threshold
was exceeded and the lake shows positive evidence for seismic shaking. In contrast, when no earthquake-related deposits are
present in the lake record at the observed time, it is assumed that the intensity threshold was not reached, resulting in
negative evidence for seismic shaking as input for the calculation of plausible magnitudes and source areas. For the studied
165 lakes in Tyrol, the intensity threshold is defined to seismic intensity (SI) $\sim VI\frac{1}{4}$ on the European macroseismic scale (EMS-
98; Grünthal, 1998) representing the mean value of the lake's individual threshold intensities (Oswald *et al.*, 2021a, 2021b).



This intensity threshold is also similar to the threshold value $VI\frac{1}{2}$ established for swiss peri-alpine lakes (Kremer et al., 2017), which further justifies to apply the estimated threshold value $SI \sim VI\frac{1}{4}$ to all studied lakes for the reconstruction of paleo-earthquake scenarios. In a first step of the grid-search analyses, minimum magnitudes are calculated for each cell based on the positive earthquake evidence. In a second step, each cell is evaluated for the sites with negative evidence and rejected if the calculated site intensity from the magnitude of the cell exceeds the intensity threshold of a site with negative earthquake evidence (see also Kremer et al., 2017).

3.4 Calculation of paleo-earthquake shakemaps

For a deterministic presentation of the paleo-earthquake effects, we created shakemaps to show the expected seismic intensity (EMS-98) in the broader study area for selected paleo-earthquake scenarios. Therefore, we used the empiric intensity (I) – distance (d) relation (equation 4) for earthquakes in Central Europe by Sponheuer (1960):

$$I(d) = I_0 - 3 \log_{10} \left(\frac{\sqrt{h^2 + d^2}}{h} \right) - 1.3 \alpha (\sqrt{h^2 + d^2} - h) \quad (4)$$

with an absorption coefficient α (0.002 for earthquakes in Central Europe) and the expected maximum intensity I_0 from the empiric relation by Rudloff & Leydecker (2002) using estimated local magnitudes (M) and hypocentral depths (h) in equation (5):

$$I_0 = \frac{M + 0.154 - (0.555 \log_{10}(h))}{0.636} \quad (5)$$

As these relations do not describe site effects that contribute to the expected intensity in the study area, we used the macroseismic data from regional earthquakes of central Europe recorded between 2013 and 2020 to determine site parameters a and b for each point x that describe the median intensity difference from the empirical relation (equation 6). In a second step, we used the intensities of historical earthquake with $M_w > 5$ in Tyrol (Stucchi et al., 2013) to estimate the difference I_d of the maximum intensity to the empirically calculated I_0 . The resulting equation has the form:

$$I(x) = I(d) + a(M, h, d) b(x) + I_d \quad (6)$$

While parameter a is depending on earthquake parameters, b relates to local topographic effects taken from a 1 km resolution digital elevation model. Therefore, uncertainties can be expected for topographic features < 1 km especially narrow valleys.

4 Results

4.1 Prehistoric earthquake records in Tyrol

4.1.1 Extension of the paleoseismic records at Plansee and Achensee

Seismic data of Plansee holds eleven seismic-stratigraphic horizons of coeval, multiple MTDs (A-K in Fig. 2A), of which the upper five each correspond to an amalgamated turbidite in the sediment core (Oswald et al., 2021b). As this assemblage



195 of observational evidence for horizon A, is linked to the severe, historic M_w 5.3 Namlos earthquake, also horizons B-E were interpreted as earthquake-induced mass-wasting events (Oswald et al., 2021b). Towards greater depths six additional horizons of coeval, multiple MTDs occur in seismic data (F-K in Fig. 2A), each containing 3 to 5 MTDs in the main basin of Plansee (see supplementary information of Oswald et al. 2021b).

In the sediment core, two main types of turbidites thicker than 5 cm are observed in the glaciolacustrine clays and mapped throughout the core (Fig. S2). The first turbidite type is characterized by brown to light grey colored, normal graded deposits with a distinct light-colored clayey silt cap on top and contains terrestrial macro-organic remains (Fig. 2b). In analogue to the lacustrine sedimentation, these graded turbidites are interpreted to result from lake-external detrital sediment transported into the lake during hydrological events (Kiefer et al., 2021). The second type consists of overall grey homogeneous turbidites with only a thin graded base and a distinct clayey-silt cap on top and without any macro-organic remains (Fig. 2c). These homogeneous turbidites are interpreted as sediment remobilization of lake-internal slopes. The turbidite of event J contains a 5 cm, angular dolomite gravel within a homogeneous silt matrix in the uppermost part. This gravel potentially indicates a dropstone transported within a snow avalanche on a frozen lake (cf. Vasskog *et al.*, 2011). Additionally, based on core-to-seismic correlation, each of the seismic-stratigraphic horizons H-J correspond to a homogeneous turbidite in the 15 m long sediment core (Fig. 2a). Therefore, we interpret these homogeneous turbidites derived from lake-internal enhanced mass wasting as earthquake-related in analogue to the earthquake proxy in the Holocene lacustrine sediments in Plansee (Oswald et al., 2021b) and similar lake settings (e.g. Strasser *et al.*, 2013). In contrast, seismic-stratigraphic horizons F and G correlate to a single or a sequence of graded and much thinner turbidites separated by background sediment (Fig 2a-b). The interpretation of seismic stratigraphic horizons F and G is not unique and they could either represent earthquakes with potentially lower intensities at the lake or hydrological events that caused onshore mass wasting within a short period. Therefore, event horizons F and G are not further used for the paleoseismic catalogue of the region.

215 The pre-existing age-depth model covering the Holocene is extended towards the base of glaciolacustrine sediments by adding an additional radiocarbon age in the Late Glacial at 7.5 m event-free sediment depth (Table S1; Fig. S2) and an inferred deglaciation age at circa 15-17 ka BP at 13.5 m (Ivy-Ochs et al., 2008). This results in paleo-earthquakes at circa 12.7, 13.4, 14.6 and 16.0 ka BP with 95% age ranges of 12.5-12.9, 13.3-13.6, 14.3-14.9 and 15.6-16.4 ka BP, respectively (Table 1).

Achensee contains twelve seismic-stratigraphic horizons with multiple MTDs, delta collapse deposits and (mega-)turbidites (A-L in Fig. 3a; Oswald *et al.*, 2021a). Similar to Plansee, sedimentary earthquake imprints are expressed by the occurrence of multiple, coeval MTDs in seismic data and a corresponding amalgamated turbidite was previously correlated to the historical severe M_w ~5.7 Hall earthquake in 1670. Therefore seismic-stratigraphic horizons B-L were interpreted as earthquake-related, but only a rough age estimate (11 – 18 ka BP) was provided for the event horizons K and L which are below the reach of the sediment cores. In contrast, the youngest event horizon A is not earthquake-related and represents a period of enhanced shoreline erosion due to anthropogenically induced lake level changes especially at the early phase of hydropower generation at Achensee.

230

In reflection seismic data of Achensee, lake strata is offset by subaqueous surface ruptures in prolongation of an onshore mapped fault. The upper terminations of these surface ruptures occur at three different stratigraphic levels, where each

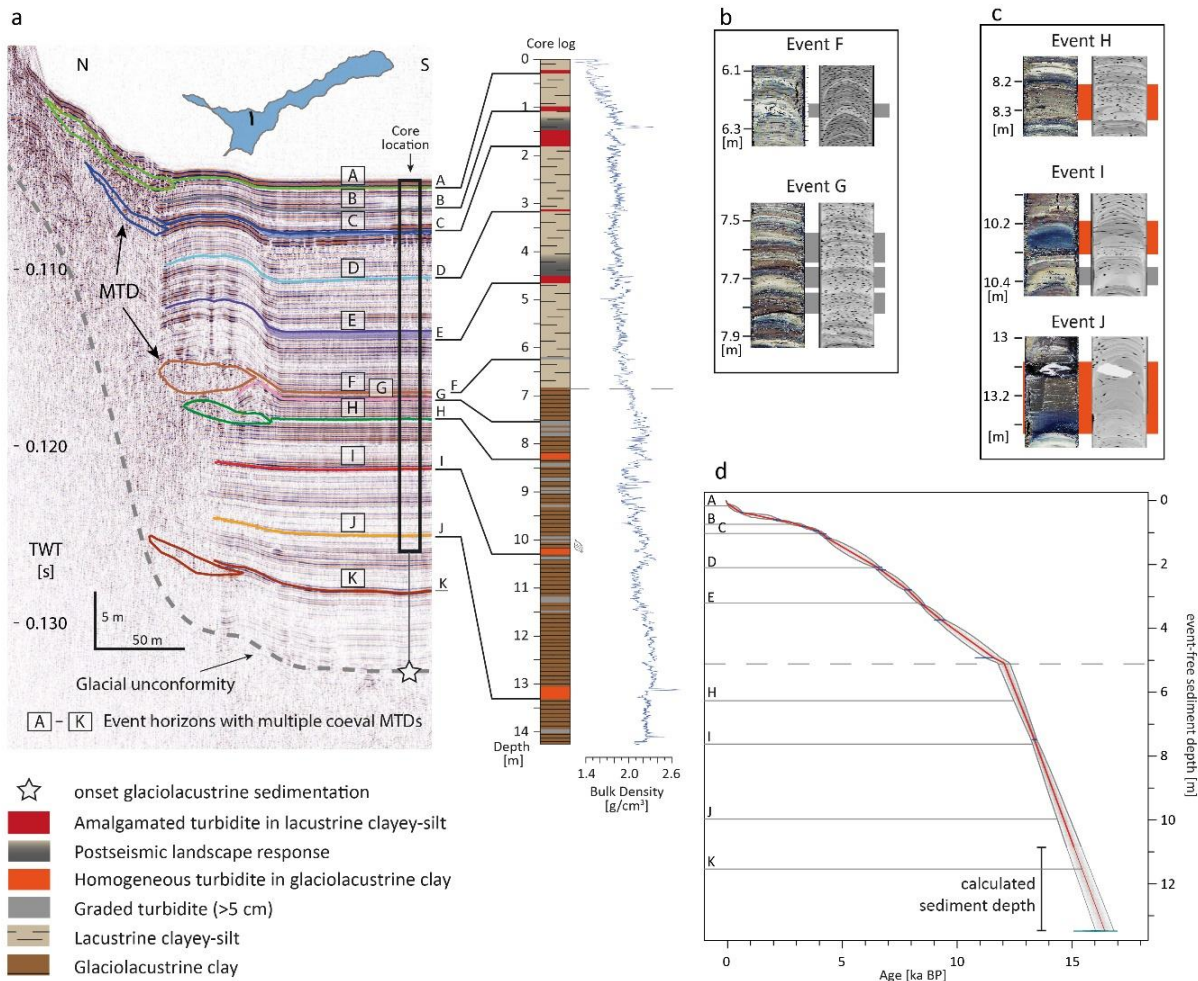


Figure 2: Extension of the paleoseismic record at Plansee. A) Core-to-seismic correlation of the seismostratigraphic event horizons with multiple coeval MTDs (I-K) in seismic data to event deposits within the glaciolacustrine sediments. Correlation of event horizons A-E with amalgamated turbidites in the sediment core are derived from Oswald *et al.* (2021b). Core depth is extrapolated below the reach of the core to the onset of glaciolacustrine sedimentation. Inset figure shows the location of the seismic line on Plansee. B) Single turbidites or a turbidite stack characterized by a normal grading and terrestrial macro-organic remains in histogram-equalized core images and CT data correlate to the seismic-stratigraphic event horizons F and G. These event horizons cannot be conclusively interpreted and either represent earthquakes or hydrological events. C) Turbidites characterized by an overall homogeneous sediment body on top of a thin normal graded base in histogram-equalized core images and CT data are correlated to the seismic-stratigraphic event horizons H-J and are interpreted as earthquake-related deposits within the glaciolacustrine sediments. D) Age-depth model of Plansee including calibrated ¹⁴C ages from this study and Oswald *et al.* (2021b; Table S1) and an assumed lake initiation age (~15-17 ka BP) derived from the regional deglaciation age (Ivy-Ochs *et al.*, 2008). Horizontal lines depict (projected) event horizons A-K. Dashed horizontal line represents the stratigraphic boundary between glaciolacustrine and lacustrine sedimentation. Sediment depth below the reach of the core (thin grey line) are calculated towards the glacial unconformity from TWT in seismic data assuming an acoustic velocity of 1,610 m/s.



235

termination is directly overlain by multiple coeval MTDs (event horizons G, K and L). This surface rupture-MTD association was previously interpreted as combined on-fault and off-fault paleoseismic evidence for three local severe earthquakes (Oswald *et al.*, 2021a). The other event horizons with multiple coeval MTDs and a corresponding turbidite were interpreted as the record of remote earthquakes exceeding the intensity threshold at Achensee SI ~VI. So far, eight of the eleven seismic-stratigraphic horizons with multiple MTDs (B-I) and one surface-rupturing horizon (G) are cored and dated by two 11 m long sediment cores. The extension of the age-depth model results in two local surface-rupturing events at ~11.0 and ~11.5 ka BP (K and L) and a remote earthquake at ~10.8 ka BP with 95% age ranges of 10.6-11.5, 11.0-11.9 and 10.4-11.2 ka BP, respectively (Table 1).

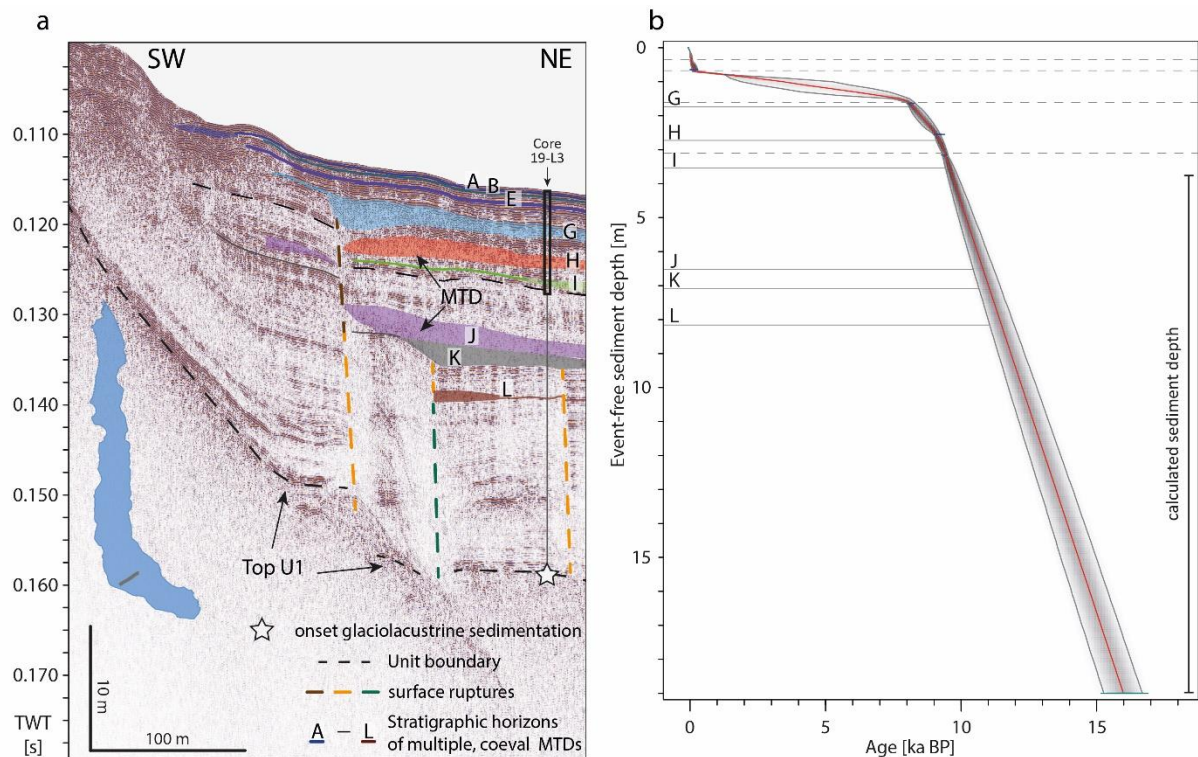


Figure 3 Extension of the paleoseismic record at Achensee. **A)** Earthquake imprints are expressed as horizons of multiple coeval MTDs and subvertical subaqueous surface ruptures (Oswald *et al.*, 2021a). The vertical thin grey line shows the prolongation of the previously published sediment core ACH19-L3 towards the interpreted onset of glaciolacustrine sedimentation at the top of unit 1. Inset shows the orientation of the seismic profile on Achensee. **B)** Extension of the age-depth model of core ACH19-L3 towards the assumed begin of glaciolacustrine sedimentation (~15-17 ka BP after Ivy-Ochs *et al.*, 2008). Projected event-free sediment depths of event horizons J-L are marked by horizontal lines. Dashed horizontal lines represent stratigraphic boundaries. The calculated event-free sediment depth results from the depth calculation between the base of the core and the interpreted onset of glaciolacustrine sedimentation of TWT in seismic data assuming an acoustic velocity of 1,610 m/s.



4.1.2 The paleo-earthquake catalogue of Tyrol and its surrounding regions

240 The sedimentary archives of Plansee, Piburgersee and Achensee represent the first continuous records of prehistoric earthquakes in the western Eastern Alps (Tyrol and its surrounding regions) and cover the last 16,000 years (Fig. 4a, Table 1). For each event, a qualitative intensity scaling is applied above the intensity threshold for recording earthquakes based on sedimentological criteria, such as MTD volume, turbidite thickness, development stage and thickness of SSDS and occurrence of postseismic landscape response (Fig. 4a; Oswald *et al.*, 2021a; b). In contrast to Plansee and Achensee, the paleoseismic record of Piburgersee is limited to the Holocene lacustrine sediments due to the lack of earthquake-induced soft-sediment deformation structures in the glaciolacustrine sediments and due to the missing seismic penetration (< 0.003 s TWT) to potentially link outstanding turbidites to multiple coeval MTDs.

The Plansee paleoseismic record (event number $n=9$) shows the most regular recurrence pattern of the investigated records being at the boundary of ‘weakly periodic’ and ‘strongly periodic’ with a mean burstiness of -0.29 (range -0.40 to -0.22 ; Fig. 3b). It also has the largest mean recurrence interval of circa 2,000 years. The Achensee paleoseismic record ($n=11$) is ‘weakly periodic’ (mean burstiness -0.20 ; range -0.32 to -0.11) with a mean recurrence interval of circa 1,100 years. For the Piburgersee record ($n=8$), aperiodicity and recurrence intervals are calculated in two ways to account for the relatively long earthquake quiescence since ~ 3.0 ka BP, once considering only the closed interevent times and a second time with assuming an imminent event next year. Both methods show a ‘weakly periodic’ to ‘aperiodic’ recurrence pattern (mean burstiness of -0.04 / -0.06 ; range -0.16 to 0.03 / -0.13 to 0.00) but vary in the recurrence interval with circa 1000 and 1250 years for the closed intervals and the imminent event next year, respectively. The ‘real’ recurrence interval at Piburgersee is potentially even longer, as the imminent event will probably be further in the future. Note that the smaller scatter of burstiness and recurrence interval in the Piburgersee dataset considering an imminent event next year is artificial due to the small age error of the assumed event in 2022 compared to the event ages derived from the individual age model simulations. Evaluating these recurrence statistics in light of the geographical position of the records within the Alpine orogen, the more externally situated Plansee shows the longest recurrence interval and most periodic recurrence pattern, whereas the more orogen-internal records (Piburgersee and Achensee) tend to aperiodic recurrence behavior with about only half of the recurrence interval at Plansee. Additionally, we combine the event ages of all earthquake-related sedimentary imprints derived from the three paleoseismic records and consider the interpreted coeval events at circa 3.0, 4.1 and 6.8 ka BP only once (Oswald *et al.*, 2021b; Fig. S3). This results in 25 severe earthquakes that occurred in the study area every 630 years on average with a weakly periodic recurrence pattern.

We examined the herein presented paleo-earthquake catalogue of Tyrol (Table 1) for further overlapping event ages, as this potentially indicates that a single event left traces in multiple lakes and thus impacted an area of several tens of km circumference. However, for overlapping event ages two or more less strong events at different locations and within a shorter time period than the error of the age-depth model are also conceivable (Kremer *et al.*, 2017; Oswald *et al.*, 2021b). For this event-age synchronicity evaluation, we incorporated the pre-existing surrounding lacustrine paleoseismic archives at

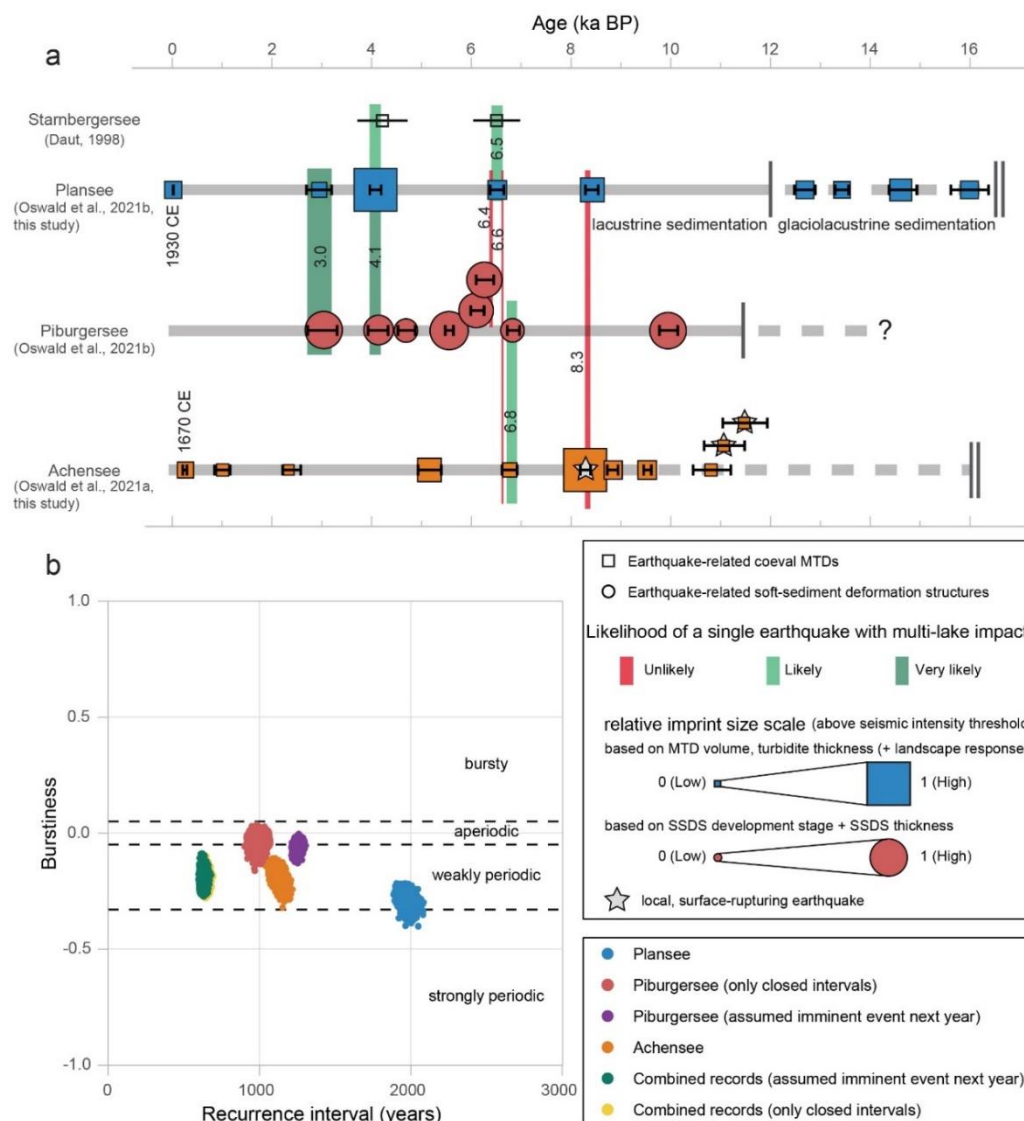


Figure 4 Lacustrine paleoseismic records of the western Eastern Alps, recurrence statistics of their paleo-earthquakes and potential single earthquakes with impact in multiple lakes. **A)** Timeline of the paleo-earthquakes at Plansee (this study and Oswald *et al.*, 2021b), Piburgersee (Oswald *et al.*, 2021b) and Achensee (this study and Oswald *et al.*, 2021a) also including the potential earthquake-related mass wasting events at Starnbergersee (Daut, 1998). Earthquake symbols are relatively scaled based on their imprint size above the EMS-98 intensity threshold for recording earthquakes at the lakes (cf. Oswald *et al.*, 2021b). Duration of lacustrine and glaciolacustrine sedimentation is indicated by continuous and dashed horizontal grey lines, respectively. The likelihood assessment that these periods represent single earthquakes with an impact in multiple lakes (green colour scale) is based on age overlaps of the individual event age PDFs (Fig. S3) and sedimentological evidence further described in the main text. **B)** Recurrence interval-burstiness diagram of the three records calculated on all individual age-depth model simulations at the respective lake resulting in >5400 data points for each record. The recurrence interval varies from circa 1000 to 2000 years for the individual records and is circa 680 years for all three records combined. The burstiness shows weakly periodic to aperiodic recurrence patterns for all data sets. Note that Piburgersee is considered as two data sets given the long open end since the last event: one data set where only the closed interevent times were considered and a second data set where an imminent event is assumed in the next year.



the lakes Constance (Schwestermann, 2016), Zürich (Strasser et al., 2013; Strasser and Anselmetti, 2008), Walen (Zimmermann, 2008), Silvaplana (Bellwald, 2012), Iseo (Lauterbach et al., 2012) and Ledro (Simonneau et al., 2013) for a potential event age overlap, but found only negative evidence for overlapping event ages with the three Tyrolean lakes. Moreover, the sedimentary archive of Ammersee, which was primarily investigated for its flood record, holds no paleoseismic events in the available core data of the last ~5.7 kyrs (Czymzik et al., 2013). At Starnbergersee, limnogeological investigations found enhanced mass wasting in seismic and core data at around 4 ka BP (3.7 to 4.7 ka BP) and in the Early Atlantic (circa 6.5 ± 0.5 ka BP; Daut, 1998). As the establishment of a continuous paleoseismic record was not the focus of the study at Starnbergersee, we only consider the two mass wasting events at circa 4 and 6.5 ka BP as potential evidence for seismic shaking (Fig. 4a), but do not extract negative evidence from this record. The paleoseismic event catalogue of the western Eastern Alps holds six periods with overlapping event ages in two records at circa 3.0, 6.4, 6.5, 6.6, 6.8 and 8.3 ka BP and one period at circa 4.1 ka BP with overlapping event ages in three records (Fig. 4a). A single severe event with impact in multiple lakes is very likely for the events at ~3.0 (Plansee, Piburgersee) and ~4.1 ka BP (Plansee, Piburgersee and potentially Starnbergersee), because the 95% PDFs of the event age ranges at Plansee and Piburgersee match well with 55% and 45%, respectively (Oswald *et al.*, 2021b; Fig. S3). Additionally, potential terrestrial secondary paleoseismic evidence is documented during these periods by the occurrence of several large prehistoric rockslides (up to 1×10^9 m³ rockslide deposit volume; Prager *et al.*, 2008; Oswald *et al.*, 2021b). Furthermore, a single earthquake at circa 6.8 ka BP is indicated by a 68% PDF event age overlap between lakes Piburgersee and Achensee (Fig. 4a). In the time period of ~8.3 ka BP the PDF event age overlap at the lakes Achensee and Plansee is low (19%) and also the observational evidence contradicts the possibility of a single event at this time. In detail, the rupture location is restricted to the Achensee area based on primary paleoseismic evidence. Within the same period, seismic shaking beyond the EMS-98 intensity threshold is indicated at Plansee by extensive mass-wasting and the occurrence of postseismic landscape response, but no earthquake-related sedimentary imprint is found at Piburgersee. We also propose to reject the possibility of a single earthquake with an imprint in multiple lakes at circa 6.4 (Piburgersee-Plansee) and 6.6 ka BP (Plansee-Achensee) due to the poor PDF event age overlap of 6% and 4%, respectively.

4.2 Potential scenarios of paleo-earthquakes

Based on the interpreted coeval earthquake evidence in multiple lakes at circa 3.0, 4.1, 6.5, and 6.8 ka BP, we investigate assemblages of potential source area and magnitude for these events under the assumption of a single earthquake event based on a reverse application of the IPE in a geospatial analysis (Fig. 5). For the following scenarios, the surrounding paleoseismic archives of the lakes Constance, Zürich, Walen, Iseo, Ledro, Silvaplana and Ammersee (for the last ~5.7 kyrs) were applied as negative earthquake evidence due to missing event-age overlap or no earthquake imprints at all in the case of Ammersee.



305 **Tabelle 1: Paleoseismic events of the western Eastern Alps, their sedimentary imprints in the lakes Plansee, Piburgersee and Achensee and the calculated relative imprint size scale**

Lake	Earthquake ID	Event horizon	Core depth [cm]	Event corrected depth [cm]	Modelled event ages [cal a BP]				off-fault paleoseismic evidence				on-fault		Reference			
					mean	from	to	%	Turbidite / SSSDs thickness [cm]	MTD amount	MTD volume [m ³]	Megaturbidite volume [m ³]	Postseismic landscape re-emergence	SSDS type		subaqueous surface rupture	Qualitative earthquake intensity	
Plansee	EQ-A	A	21	16	20	-	-	-	-	8	$\frac{1}{2}$	21,000	-	-	-	-	0.16	Oswald et al. (2021b)
Plansee	EQ-B	B	96.5	73	2948	2691	3196	95	9	9	8,000	-	-	-	-	-	0.09	Oswald et al. (2021b)
Plansee	EQ-C	C	142.5	102	4076	3961	4187	95	37	$\frac{1}{0}$	100,000	-	yes	-	-	-	1.00	Oswald et al. (2021b)
Plansee	EQ-D	D	310.5	209	6515	6372	6649	95	4	$\frac{5}{6}$	40,000	-	-	-	-	-	0.24	Oswald et al. (2021b)
Plansee	EQ-E	E	448.5	320.5	8422	8283	8543	95	16.5	6	17,000	-	yes	-	-	-	0.43	Oswald et al. (2021b)
Plansee	EQ-H	H	821	626.5	12693	12471	12891	95	15	5	3,700	-	-	-	-	-	0.10	this study
Plansee	EQ-I	I	1032	762	13436	13288	13560	95	12	3	6,600	-	-	-	-	-	0.10	this study
Plansee	EQ-J	J	1312.5	998.5	14645	14370	14930	95	24	2	5,000	-	-	-	-	-	0.16	this study
Plansee	EQ-K	K	not cored	1259.5	15982	15611	16363	95	15	3	3,900	-	-	-	-	-	0.10	this study
Piburgersee	EQ-1	1	344	75.5	3039	2716	3306	95	9	-	-	-	-	-	intraclast breccia	-	0.98	Oswald et al. (2021b)
Piburgersee	EQ-2	2	376.5	95.5	4133	3927	4327	95	5	-	-	-	-	-	incipient breccia	-	0.63	Oswald et al. (2021b)
Piburgersee	EQ-3	3	458	108	4681	4528	4871	95	4	-	-	-	-	-	folded layer	-	0.35	Oswald et al. (2021b)
Piburgersee	EQ-4	4	493.5	132.5	5550	5474	5636	95	10	-	-	-	-	-	intraclast breccia	-	1.00	Oswald et al. (2021b)
Piburgersee	EQ-5	5	517	148.5	6092	5987	6252	95	2	-	-	-	-	-	intraclast breccia	-	0.80	Oswald et al. (2021b)
Piburgersee	EQ-6	6	530.5	154	6258	6093	6445	95	4	-	-	-	-	-	intraclast breccia	-	0.85	Oswald et al. (2021b)
Piburgersee	EQ-7	7	554.5	172.5	6823	6716	6964	95	5	-	-	-	-	-	folded layer	-	0.38	Oswald et al. (2021b)
Piburgersee	EQ-8	8	654.5	265	9939	9767	10133	95	6	-	-	-	-	-	intraclast breccia	-	0.90	Oswald et al. (2021b)
Achensee	B	B	86*	57*	267	213	296	95	22*	$\frac{1}{2}$	50,000	-	-	-	-	-	0.02	Oswald et al. (2021a)
Achensee	C	C	225*	151*	1012	849	1164	95	13*	8	15,400	-	-	-	-	-	0.01	Oswald et al. (2021a)
Achensee	D	D	279*	200*	2337	2213	2578	95	9*	6	10,300	-	-	-	-	-	0.01	Oswald et al. (2021a)
Achensee	E	E	386*	275*	5157	4930	5394	95	45*	$\frac{1}{2}$	165,400	50,200	-	-	-	-	0.07	Oswald et al. (2021a)
Achensee	F	F	505*	321*	6768	6611	6913	95	18*	8	45,600	-	-	-	-	-	0.02	Oswald et al. (2021a)
Achensee	G	G	654*	382*	8278	8180	8387	95	83*	5	3,404,600	189,500	-	-	-	Yes	1.00	Oswald et al. (2021a)
Achensee	H	H	757*	427*	8838	8723	8938	95	15*	9	648,700	-	-	-	-	-	0.18	Oswald et al. (2021a)
Achensee	I	I	859*	489*	9520	9449	9604	95	15*	6	683,900	24,900	-	-	-	-	0.20	Oswald et al. (2021a)
Achensee	J	J	1305**	653**	10802	10442	11198	95	10**	3	111,500	-	-	-	-	-	0.03	this study
Achensee	K	K	1415**	708**	11052	10664	11475	95	10**	4	96,800	-	-	-	-	Yes	0.03	this study
Achensee	L	L	1632**	816**	11465	11037	11929	95	10**	5	57,200	-	-	-	-	Yes	0.02	this study

* derived from longcore ACH19-L7 in the main basin

**event layer not cored: extrapolated depth values or assumed thickness values for qualitative intensity scaling



Scenario A at ~3.0 ka BP

Positive earthquake evidence is present in Plansee and Piburgersee at ~3.0 ka BP, whereas Achensee, Ammersee and the Swiss and Italian paleoseismic archives show negative evidence (Fig. 5b). The grid-search analysis provides solutions of potential earthquake sources in the western study area with a minimum magnitude source area in the middle between Plansee and Piburgersee around the village Nassereith with M_w 5.7 (Fig. 5b). The large prehistoric rockslides at Tschirgant and Haiming indicated as violet triangles in Fig. 5b also fall within the time range of this event and were interpreted to be earthquake triggered (Oswald et al., 2021b). These rockslides are located slightly south of the minimum magnitude area and much closer to Piburgersee than to Plansee. Additionally, the relative scaling of the sedimentary imprint size (0.98 at Piburgersee and 0.11 at Plansee; Table 1) indicates a much higher shaking intensity at Piburgersee than at Plansee. Therefore, we interpret the epicenter of scenario A to be more likely located south of the halfway distance between the two lakes (white line in Fig. 5b) with a minimum magnitude of M_w 5.8. Hereinafter we consider M_w 5.8 as minimum magnitude for scenario A and use this value for further considerations and analyses (sect. 4.3).

Scenario B at ~4.1 ka BP

At ~4.1 ka BP, positive earthquake evidence is found in Plansee and Piburgersee and potentially in Starnbergersee, whereas Achensee, Ammersee and the Swiss and Italian lakes show negative evidence for seismic shaking (Fig. 5c). The rockslides at Fernpass, Eibsee and Stöttelbach (violet triangles in Fig. 5c) were previously related to this earthquake (Oswald et al., 2021b). Moreover, results from structural analyses and rock slope failure modelling in response to seismic shaking also suggest a seismic trigger for the Fernpass rockslide (Lemaire et al., 2020). The derived minimum-magnitude and source area lies north of Garmisch-Partenkirchen with a magnitude of M_w 6.1. This event had the largest sedimentary imprint at Plansee (relative imprint scale = 1) but had only an intermediate imprint size in Piburgersee (relative imprint scale = 0.63; Table 1). This observational evidence further supports that the localization of the already small region of plausible source areas and minimum magnitudes from the grid-search analysis (Fig. 5c). It must be noted, that this analysis strongly relies on the less constrained evidence at Starnbergersee. Not considering Starnbergersee as a datapoint would result in the same magnitude-source area distribution as in scenario A (Fig. 5b), but resulting in a minimum magnitude estimate of M_w 6.0 around Plansee and the rockslides at ~4.1 ka BP considering the sedimentary imprint size and the locations of the earthquake-triggered rockslides (see argumentation above).

Scenario C at ~6.5 ka BP

Plansee and potentially Starnbergersee have positive evidence for seismic shaking at ~6.5 ka BP and negative evidence is found in the other available records (Fig. 5d). The region north of Garmisch-Partenkirchen is a potential source area with a minimum magnitude of M_w 5.9, centrally located between the two lakes, or increasingly higher, if the epicenter would have been located further towards the north, west or south. Better constraining the epicenter based on the sedimentary imprint is not feasible for this event, as there is no data on the imprint size at Starnbergersee. However, the low imprint size in Plansee (0.11; Table 1) hints at an earthquake which occurred farther away. Therefore, we assume the identified minimum magnitude

340

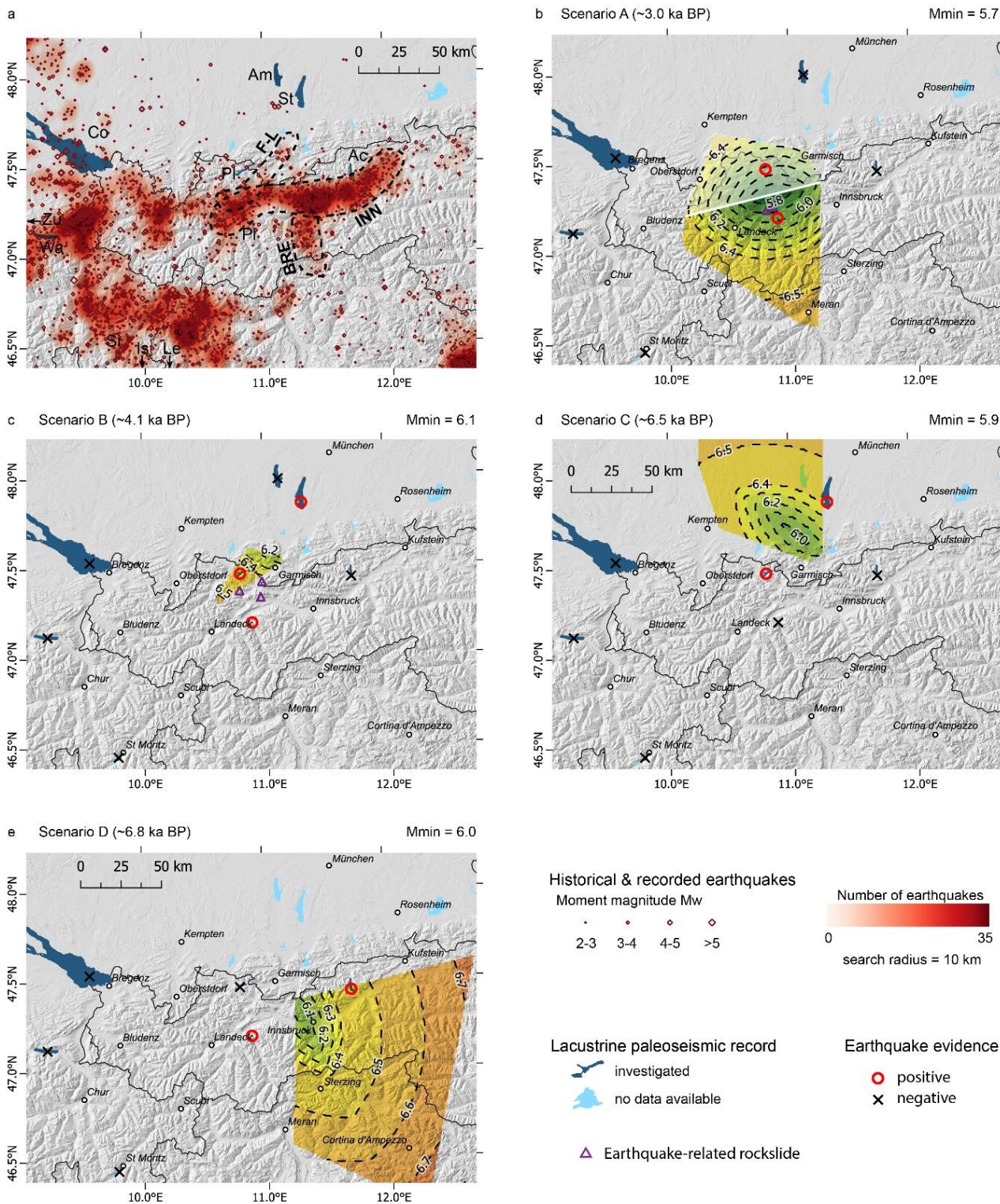




Figure 5 Magnitude and source area estimations of plausible paleo-earthquake scenarios with considering positive and negative earthquake evidence at multiple sites reversely using an IPE in a grid-search analysis (Strasser *et al.*, 2006; Kremer *et al.*, 2017, after Bakun & Wentworth, 1997). a) Map with historical and instrumentally-recorded earthquake data (Stucchi *et al.*, 2013; Reiter *et al.*, 2018), zones of present-day enhanced seismicity (dashed lines) around the Inn valley (INN), the Brenner pass (BRE) and the Fernpass-Loisach region (F-L). The lacustrine event records investigated for the scenario modelling are Achensee (Ac; Oswald *et al.*, 2021a), Ammersee (Am; Czymzik *et al.*, 2013), Lake Constance (Co; Schwestermann, 2016), Lake Iseo (Is; Lauterbach *et al.*, 2012), Lake Ledro (Le; Simonneau *et al.*, 2013), Piburgersee (Pi; Oswald *et al.*, 2021b), Plansee (Pl; Oswald *et al.*, 2021b), Silvaplansee (Si, Bellwald, 2012), Starnbergersee (St, Daut, 1998), Walensee (Wa; Zimmermann, 2008); Lake Zürich (Zu; Strasser & Anselmetti, 2008; Strasser *et al.*, 2013). b-f) Calculated plausible source areas and minimum magnitudes for paleo-earthquakes with assumed coeval positive earthquake evidence in more than one lake at b) ~3.0 ka BP, c) ~4.1 ka BP, d) ~6.5 ka BP, e) ~6.8 ka BP. In b) and c) the interpreted earthquake-related rockslides are indicated as violet triangles (Oswald *et al.*, 2021b). Note that in b) the transparent source area north of the white line are less likely due to the relatively large sedimentary imprint in Piburgersee compared to Plansee and the the earthquake-triggered rockslides further support this interpretation. Hence, the estimated source area is interpreted more in the south with a minimum magnitude of M_w 5.8, which is also used for further considerations and analysis.

area to be the most likely epicenter location for this event. Similar to scenario B, the grid-search analysis strongly relies on the less constrained evidence in Starnbergersee. In the case of a false interpreted evidence in Starnbergersee for this event, the minimum magnitude area would shift towards Plansee.

345 **Scenario D at ~6.8 ka BP**

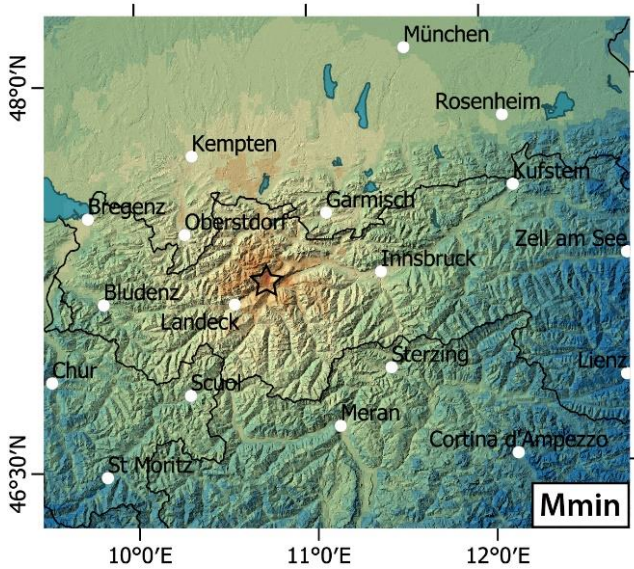
At ~6.8 ka BP positive earthquake evidence is found in Achensee and Piburgersee, whereas negative evidence is derived from Plansee (Fig. 5e). The minimum magnitude source area is located around Innsbruck with a minimum magnitude estimate of M_w 6.0 and with increasing magnitudes towards the east and southeast. As both Achensee and Piburgersee have only minor sedimentary imprints sizes for this event (0.11 and 0.38, respectively; Table 1), an epicenter location farther
350 away from both record like the area of Innsbruck or south of it is most likely.

4.3 Effects of selected paleo-earthquakes

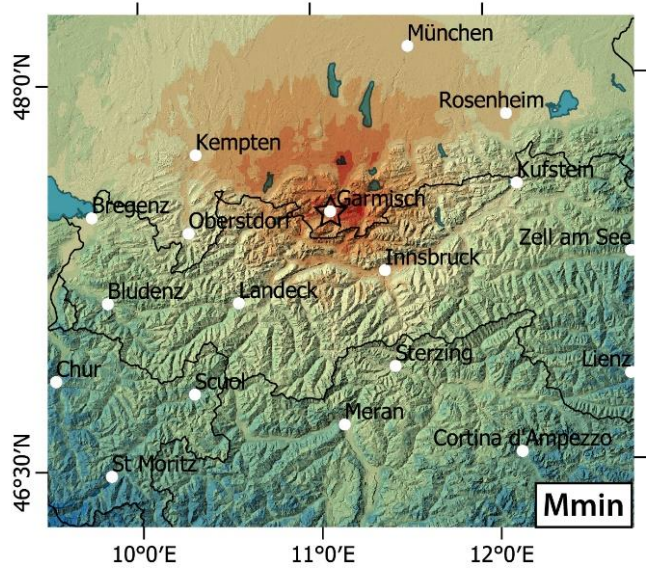
The derived magnitudes from the modeled paleo-earthquake scenarios are well above what has been calculated from instrumental earthquake records of the last century or from historical documentation in the study area. To get a first-order idea of the consequences of such rare high-magnitude events, we explore the regional shaking effects of four selected paleo-earthquake scenarios, which are reasonably constrained by our lacustrine paleoseismic data. The epicenter location of the
355 earthquake scenarios for the circa 3.0, 4.1 and ~6.8 ka events are estimated based on the minimum magnitude source area as revealed from the grid-search analysis. In a second step, the epicenter locations are considered more plausible closer to earthquake-triggered rockslides and lakes with higher sedimentary imprint scales (see sect. 4.2). For the estimated epicenter area, we take the nearest city and derive the magnitude calculated from the inverse application of IPE in the grid-search
360 analysis for the respective paleo-earthquake scenario. Besides the exploration of regional shaking effects for plausible earthquake scenarios at circa 3.0, 4.1 and ~6.8 ka BP, we test for the maximum possible magnitude of the surface-rupturing earthquake at Achensee at ~8.3 ka BP, that did not exceed the EMS-98 intensity threshold at Piburgersee and Plansee. A



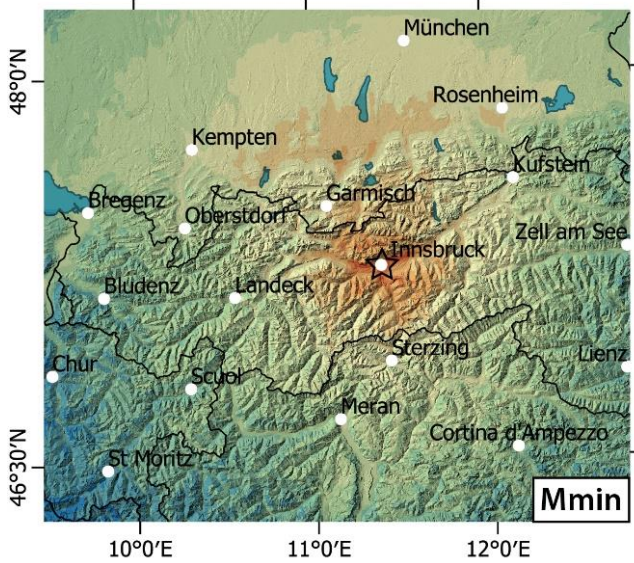
a M_w 5.8 near Imst Scenario A (~3.0 ka BP)



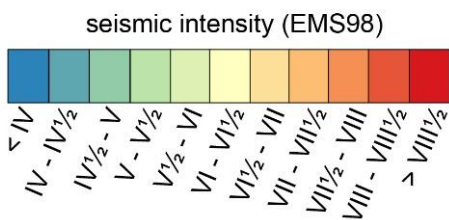
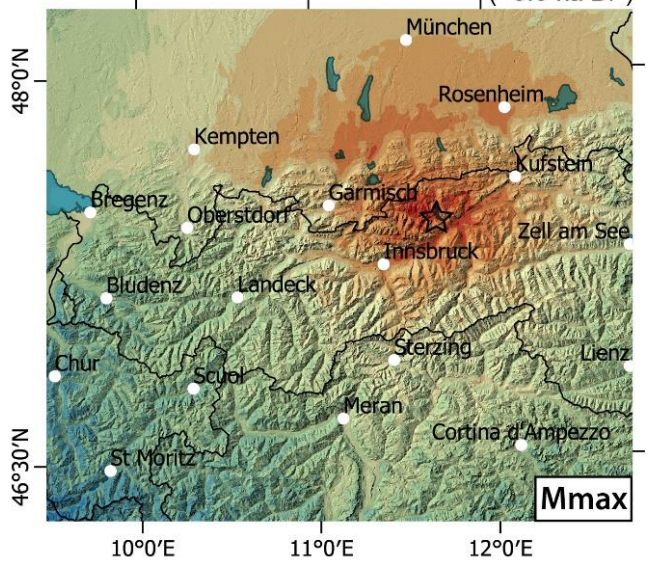
b M_w 6.1 near Garmisch Scenario B (~4.1 ka BP)



c M_w 6.0 near Innsbruck Scenario D (~6.8 ka BP)

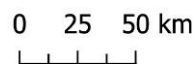


d M_w 6.3 at Achensee surface-rupturing event (~8.3 ka BP)



☆ epicentral location

lakes



Mmin Minimum magnitude required to generate the observed lake paleoseismic evidence

Mmax Maximum possible magnitude at Achensee with negative evidence in the other lakes



Figure 6 Shakemaps of selected paleo-earthquake scenarios. Magnitudes and epicentral location are based on the calculated source areas and minimum magnitudes and evaluation based on the relative size of the earthquake-related sedimentary imprint and the location of earthquake-triggered rockslides (see section 4.2). The shakemaps show seismic intensities (EMS-98) calculated for the minimum magnitude estimates of the paleo-earthquakes with presumed epicenters a) near Imst at ~3.0 ka BP, b) close to Garmisch-Partenkirchen at ~4.1 ka BP, c) near Innsbruck at ~6.8 ka BP. In contrast, d) presents the maximum possible magnitude of MW 6.3 for a surface-rupturing earthquake at Achensee without exceeding the seismic intensity threshold at Plansee and Piburgersee. The shakemaps are based on empirical relations of intensity-to-distance (Sponheuer, 1960) and magnitude-to-epicentral intensity (Rudloff & Leydecker, 2002), modified by macroseismic data of recorded earthquakes and epicentral intensities of historical events, and corrected for topographic effects. The calculated seismic intensities at major towns for the different paleo-earthquake scenarios are provided in Table 2.

365 focal depth of 10 km is assumed for calculating the shakemaps presented in Fig. 6, which lies within the 5-15 km depth range of recent seismicity (Reiter et al. 2018). The respective calculated seismic intensities for selected towns in the broader study area are listed in Table 2.

Effects of a M_w 5.8 earthquake at Imst (Scenario A at ~3 ka BP)

370 A M_w 5.8 earthquake scenario at Imst would have an epicentral intensity of VIII^{1/4} and the earthquake would affect large parts of Tyrol and also areas of southern Bavaria, Baden-Württemberg and Vorarlberg (Fig. 6a). Especially western Tyrol and the northern Alpine foreland from Kempten to Starnbergersee would be strongly affected (SI: VI to VII) in a total area of circa 9,000 km². The very strongly affected area with intensities >VII (~550 km²) is found around the epicenter.

Effects of a M_w 6.1 earthquake at Garmisch (Scenario B at ~4.1 ka BP)

375 A M_w 6.1 earthquake scenario at Garmisch would have an epicentral intensity of VIII ^{3/4} and would affect large parts of Tyrol and southern Germany (Fig. 6b). In detail, the earthquake would be strongly felt in an area of circa 20,000 km² ranging from most of Tyrol up north to Augsburg and from lake Constance to Chiemsee. The very strongly affected area (SI: VII-VIII) would be expected in an area of circa 5,200 km² located in the Alpine foreland from Kempten to almost Tegernsee, up north to Ammersee, and also in the Inn and the Wipp valley towards the south. Severe seismic shaking is expected around
380 the epicenter in an area of circa 270 km².

Effects of a M_w 6.0 earthquake at Innsbruck (Scenario D at ~6.8 ka BP)

A M_w 6.0 earthquake scenario at Innsbruck would have an epicentral intensity of VIII^{1/2} and would be felt in whole western Austria, Bavaria and South Tyrol (Fig. 6c). An area of circa 14,300 km² are expected to be strongly affected by seismic shaking (SI: VI-VII) especially in the Inn valley, but also in the Alpine foreland from Kempten to Rosenheim. Within an
385 area of 1,300 km² in central Tyrol would experience very strong seismic shaking (SI: VII-VIII) and severe seismic intensities (SI >VIII) are expected in the Inn valley in the area of the epicenter (~65 km²).

Investigation of the maximum possible magnitude for the surface-rupturing earthquake at Achensee at ~8.3 ka BP

As the ~8.3 ka BP surface-rupturing event at Achensee is not recorded in Piburgersee or Plansee, we estimate its maximum possible magnitude by considering that the threshold intensities at Piburgersee and Plansee were not exceeded. These
390 conditions are met for an earthquake at Achensee with a magnitude of M_w 6.3, which defines the maximum possible magnitude for the ~8.3 ka surface-rupturing event. Such an event would have an epicentral intensity of VIII ^{3/4} and would



395 affect large parts of western and central Austria, Bavaria and parts of South Tyrol (Fig. 6d). In total about 30,000 km² are
expected to be strongly affected (SI: VI-VII). In large parts of the Inn valley and southern Bavaria (circa 8,500 km²) very
strong seismic intensities (SI: VII-VIII) are expected and severe shaking (SI >VIII) would occur in circa 540 km² located in
the Achensee region and the adjacent Inn- and Ziller valleys. Surface ruptures are commonly present for $M_w > 6.0$
earthquakes (Stirling et al., 2002), which provides a minimum magnitude estimate for the surface-rupturing events at
Achensee (Oswald et al., 2021a). In combination with the maximum possible magnitude from the shakemap (Fig. 6d) the
magnitude range for the ~8.3 ka BP surface-rupturing event at Achensee is bracketed to M_w 6.0-6.3.

5. Discussion

400 5.1 Extension of paleoseismic records to Late Glacial times

In both Plansee and Achensee, the different lithologies and sedimentation rates of the glaciolacustrine and the lacustrine
sediments may also affect the sensitivity of the lake acting as a natural seismograph. The earthquake proxy of multiple
MTDs with a corresponding turbidite cannot be validated by historical events onsite for the glaciolacustrine sediments from
Late Glacial times. However, similar signatures have been successfully validated as proxies for seismic shaking in actual
405 proglacial lakes in Alaska (Van Daele et al., 2019; Praet et al., 2017), which could be seen as analogues for the Late Glacial-
Achensee and -Plansee. Increased sedimentation rates as present in the glaciolacustrine sediments might increase the
sensitivity of the subaqueous slopes to failure (Chassiot et al., 2016; Wilhelm et al., 2016), which implies a lower intensity
threshold to record seismic shaking (Praet et al., 2017). This in turn could lead to a misinterpretation of increased seismicity
within Late Glacial times, as cause for the high event frequency in the Late Glacial Plansee record (circa 820 years
410 recurrence rate). It can be assumed that seismicity in the western Eastern Alps was enhanced in Late Glacial-Early Holocene
times due to post-glacial unloading and following isostatic rebound, as interpreted in other formerly glaciated regions (Beck
et al., 1996; Bellwald et al., 2019; Brooks and Adams, 2020; Strasser et al., 2013). In contrast, sedimentary imprints of
earthquakes might be misinterpreted as hydrological event layers in the glaciolacustrine sediments due to the failure of
slopes predominantly influenced by clastic sedimentation. This makes it challenging to distinguish turbidites that originate
415 from in-lake remobilization versus external fluvial sources (Praet et al., 2020). Despite the uncertainties of potential temporal
changes in the intensity threshold and a potential incomplete earthquake record, the expansion of continuous paleoseismic
records to their longest-possible extent is especially valuable in intraplate tectonic settings where recurrence rates are long
and paleoseismic event number is typically low, and thus little knowledge is available on recurrence patterns of severe
earthquakes.

420



Table 1: Seismic intensities at surrounding major towns in Austria, Germany, Italy and Switzerland for the paleo-earthquake scenarios shown in Figures 5 and 6. Bold values indicate seismic intensities >VII. Bold and underlined values indicate seismic intensities >VIII.

Country	Town	EMS98-seismic intensity			
		Scenario A: M _w 5.8 at Imst	Scenario B: M _w 6.1 at Garmisch- Partenkirchen	Scenario D: M _w 6.0 at Innsbruck	M _w 6.3 at Achensee (~8.3 ka BP event)
Austria	Innsbruck	VI ¼	VII ¼	<u>VIII ¼</u>	<u>VIII</u>
Austria	Kufstein	V	VI	VI	VII ¼
Austria	Salzburg	IV ½	V ¾	V ½	VI ¾
Austria	Zell am See	IV ½	V ¼	V ½	VI ¼
Austria	Bregenz	VI	VI ¼	V ¾	VI
Austria	Landeck	VI ¾	VI	V ¾	V ¾
Austria	Lienz	IV	IV ¾	V	V ¾
Austria	Villach	III ¾	IV ½	IV ¾	V ½
Austria	Bludenz	V ¼	V ½	V	V ¼
Austria	Hallstatt	III	IV	IV	IV ¾
Germany	Rosenheim	V ½	VI ¾	VI ½	VII ½
Germany	Garmisch	VI ½	<u>VIII ½</u>	VI ¾	VII ¼
Germany	München	V ½	VI ¾	VI ¼	VII
Germany	Kempten	VI ¼	VII	VI ¼	VI ½
Germany	Augsburg	V ¼	VI ¼	V ¾	VI ½
Germany	Oberstdorf	VI ½	VI ½	VI	VI
Germany	Ingolstadt	IV ¾	V ¾	V ¼	VI
Germany	Ulm	V ¼	VI	V ¼	V ¾
Germany	Stuttgart	IV ¼	IV ¾	IV ¼	IV ¾
Italy	Sterzing	V ¾	VI	VI ½	VI ½
Italy	Meran	V ¾	V ¾	VI ¼	VI ¼
Italy	Cortina d'Ampezzo	IV ¾	V	V ½	V ¾
Italy	Belluno	IV ½	V	V ¼	V ¾
Italy	Trento	IV ¾	V	V ¼	V ½
Italy	Tolmezzo	IV	IV ½	IV ¾	V ½
Italy	Locarno	IV ½	IV ¼	IV ¼	IV ½
Switzerland	Scuol	V ½	V	V	V
Switzerland	Chur	IV ½	IV ½	IV ½	IV ½
Switzerland	St Moritz	IV ½	IV ¼	IV ¼	IV ¼



5.2 Intensity values used for the paleo-earthquake scenarios

For the calculation of potential source areas and magnitudes of paleo-earthquakes an IPE is reversely applied in a grid-search analysis using a single, uniform positive and negative intensity threshold solely on the lake records with a presumed intensity threshold of SI VI $\frac{1}{4}$. This is due to the fact that the intensity thresholds at the individual lakes could only be determined with maximum one positive evidence of a historical earthquake (Oswald et al., 2021a, 2021b). Additionally, the magnitudes of such historical earthquakes can have already relatively large uncertainties, as it is the case for the 1670 Hall earthquake (Stucchi et al., 2013), which in turn gets transferred to the intensity threshold estimation. For Piburgersee, the intensity threshold of SI VI $\frac{1}{2}$ to VII was estimated from negative evidence of the 1930 Namlos earthquake (Oswald et al., 2021b), which also corresponds to intensity thresholds obtained in similar lake settings (Monecke et al., 2004). Moreover, due to the absence of a well-documented historical earthquake that left evidence at multiple lake sites, we are not able to test the performance of the grid-search analysis using the presumed intensity threshold (Kremer et al., 2017). The earthquake-related rockslides are not included as input data points for the grid-search analysis due to their unknown and potentially very variable intensity threshold. When simply applying the environmental seismic intensity scale (ESI scale; Serva *et al.*, 2016), rockslides with deposit volumes $>10^7$ m³ would indicate a seismic intensity of X, which would contradict with the negative evidence found at Achensee in only 50 to 65 km distance to the potential source areas of the ~4.1 and ~3.0 ka BP events. This negative evidence constrains the maximum intensity at the rockslide sites to circa SI VIII $\frac{1}{2}$. Such a lower threshold for rockslide triggering can be explained by the relatively long-lasting interplay of hydromechanical and seismic preconditioning weakening the rock slope stability (Oswald et al., 2021b; Prager et al., 2008).

5.3 Discussion of the individual paleo-earthquake scenarios

The calculation of plausible source areas and minimum magnitudes of paleo-earthquakes assumes a single event with impact in multiple lakes. However, especially in the intraplate tectonic setting of the Alps earthquake successions or periods with enhanced seismicity are common, as exemplified by some of the strongest historical earthquakes that have occurred as clusters e.g. six events with magnitudes ranging from M_w 5.1-6.4 within five months in the Friuli region in 1976 (Carulli and Slejko, 2005) and two events of M_w 5.5 to 5.7 (\pm 0.4) in central Tyrol in 1670 and 1689 (Stucchi et al., 2013). The time periods between these historical earthquake successions are far below the age uncertainty of radiocarbon-based age-depth models and would remain undifferentiated unless multiple consecutive earthquake imprints can be distinguished within the sedimentary record (Wils et al., 2021). Therefore, it cannot be excluded that one or the other of the presented paleo-earthquake scenarios actually represent two or more closely spaced and consecutive earthquakes with slightly smaller magnitudes.

The proposed source areas of the scenarios A (~3.0 ka BP) and D (~6.8 ka BP) are both within the zone of present-day enhanced seismicity in the area of the Inn valley and the Brenner region (sect. 4.2 and 4.3) where large-scale fault systems

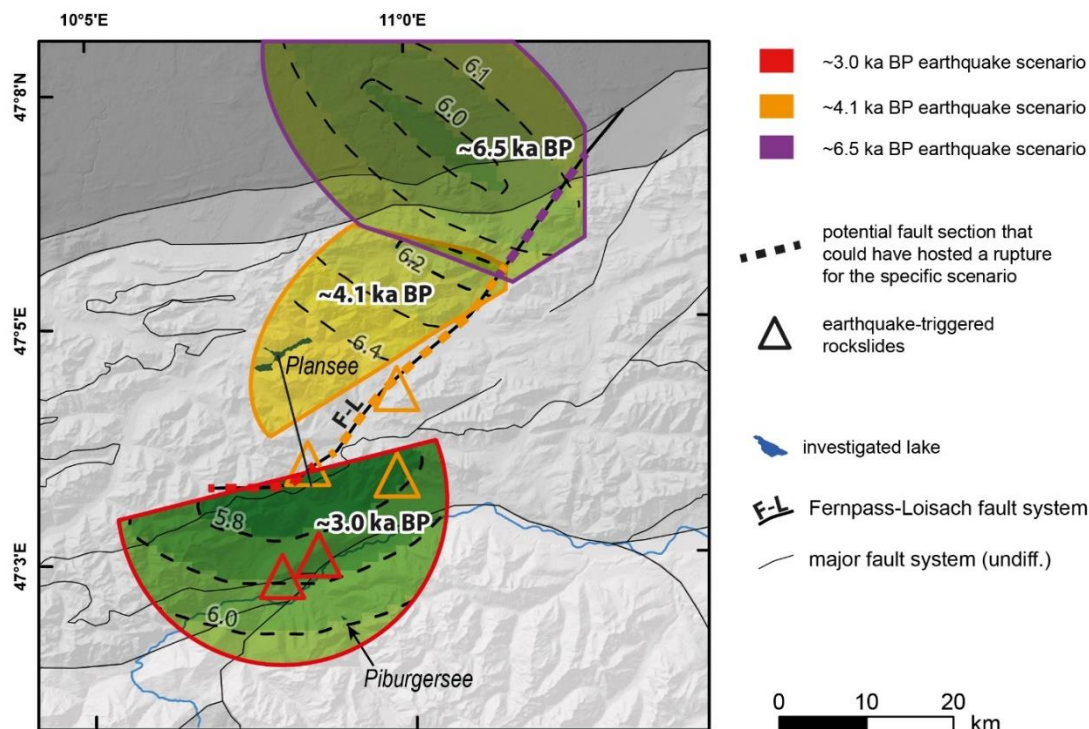


Figure 7 NE-SW migration of severe earthquakes between ~6.5 to ~3.0 ka BP (pale-earthquake scenarios A, B and C) might indicate a progressive failure of the Fernpass-Loisach fault. Solutions for the source area and minimum magnitude are derived from the inverse application of an IPE using the lacustrine paleoseismic evidence in a grid-search analysis (see section 5.2 and Figure 5.5).

are present and also severe historical earthquakes are documented (Hammerl, 2017; Stucchi et al., 2013). Therefore, we propose that the scenarios A and D are likely to have happened in these regions near Imst and Innsbruck, respectively with the calculated minimum magnitudes of M_w 5.8 and 6.0, respectively (Fig. 6). With increasing distance and magnitude, the resulting magnitudes and source area from the grid-search analysis cannot be further evaluated and narrowed down due to missing data points, which is especially the case for scenario A (towards the south; Fig. 5b) and scenario D (towards east and south; Fig. 5e). Plausible source areas of scenarios B (~4.1 ka BP) and C (~6.5 ka BP) are located at the northern part of the Fernpass-Loisach region (see considerations in sect. 4.2), which is characterized by slightly increased seismicity within the generally seismically less active Alpine front (Fig. 5a; Reiter *et al.*, 2018). It is conceivable that enough deformation is transferred towards the north and localized at this inherent, large-scale fault structure to generate severe earthquakes. However, the lack of present-day seismicity in the northern study area (Reiter et al., 2018) complicate the assessment of other potential active fault zones in the Alpine foreland despite the presence of major Alpine thrusts successively approaching the surface.



470 The shakemaps of selected paleo-earthquake scenarios provide first-order information that severe earthquakes within the
western Eastern Alps also strongly affect large areas in the northern Alpine foreland in southern Germany. Several perialpine
lakes are located in southern Germany, which are not yet studied for their potential paleoseismic records but could
essentially help in identifying more earthquake scenarios with multi-lake impact and help in better constraining epicenter
475 locations and magnitudes of the herein proposed scenarios. A previous study at Ammersee found no earthquake imprints for
the last 5.7 kyrs (Czymzik et al., 2013). This contradicts the results of the shakemaps of the paleo-earthquake scenarios (Fig.
6), where at least two events have exceeded SI VII, which is above the upper threshold value to record seismic shaking in
comparable, Swiss peri-alpine lakes (Monecke et al., 2004). Either the sediments of Ammersee have a different susceptibility
to fail during seismic shaking or event horizons of multiple mass wasting remained undiscovered due to the lack of reflection
seismic data or inadequate core siting to capture earthquake-related turbidites.

480 By taking the proposed source areas of the paleo-earthquake scenarios A, B and C (see argumentation in sect. 4.2), we
observe a spatio-temporal migration of paleo-earthquakes from NE to SW in the area of the Fernpass-Loisach fault system
(Fig. 7). When assuming these events ruptured on this fault system, this could indicate a progressive failure along this major
fault structure similar to what is observed in some transform plate boundary regions e.g. the North Anatolian fault (Stein et
al., 1997). Such stress redistribution patterns are not limited to active tectonic regions with high deformation rates, but are
485 also documented for the Friuli 1976 earthquake sequence in the Alps (Slejko, 2018). Yet, the interpretation of a progressive
failure at the Fernpass-Loisach fault system might be biased by the fact that we can only estimate source areas for paleo-
earthquakes that are recorded in at least two lakes. This interpretation ignores at least four paleo-earthquakes recorded only
in Piburgersee between the 6.5 and the 4.1 ka BP events. However, these events are likely produced by a different fault
source than the Fernpass-Loisach fault system, considering the missing coeval earthquake evidence in Plansee.

490 **5.4 Potential Implications of the paleoseismic catalogue of the western Eastern Alps**

The three presented paleoseismic archives are located at different positions within the Alpine orogeny in terms of current
seismicity (Fig. 5a), which is also reflected in their earthquake recurrence rates and patterns. We interpret the relatively
shorter recurrence rates within the more inneralpine records Piburgersee and Achensee to be related with enhanced tectonic
loading around the Inn valley also in prehistoric times. Hence, longer recurrence rates in the more external Plansee
495 potentially reflect a decreased stress transfer across the current-day enhanced seismicity zone in the south. Additionally,
recurrence behavior of the inneralpine records is slightly more aperiodic than the more external Plansee. This could reflect
different processes increasingly affecting and modulating seismicity with increasing topography and elevation in the area of
the inneralpine records, i.e. glacial isostatic adjustment, topographic potential energy or erosion (Mazzotti et al., 2020).
Especially a change of lithospheric stress due to post-glacial unloading and isostatic rebound has been previously discussed
500 to increase seismicity within the western Alps during Late Glacial to Early Holocene times (Beck et al., 1996; Kremer et al.,
2017; Strasser et al., 2013). Without being able to resolve the processes modulating seismicity, increased seismicity related



to post-glacial unloading could potentially be indicated by the increased event frequency (822 years recurrence rate) between 12 and 16 ka BP at Plansee.

In comparison to the overall aperiodic recurrence patterns of other lacustrine paleoseismic records within the Alps (Lakes
505 Cadagno, Ledro, Bohinj, Savine, Lucerne, Annecy compiled by Moernaut, 2020), the paleoseismic records of Tyrol are
slightly more periodic, but with longer recurrence rates, except lake Lucerne (recurrence interval = 2034 years, burstiness = -
0.09) which is comparable to Plansee. The slightly more periodic recurrence behavior in the Tyrolean records could be partly
artificial, as records with low event numbers tend to underestimate the burstiness and thus, tend towards a more periodic
recurrence behavior (Kempf and Moernaut, 2021; Williams et al., 2019). However, the more regular earthquake recurrence
510 pattern in Tyrol could indicate active deformation localization within one or only a few fault sources, whereas deformation
in the other alpine paleoseismic records is distributed over a complex system of interacting fault sources, which is more
typical for intraplate tectonic settings (Liu et al., 2011). In Tyrol, the circa 20 km broad and 100 km long zone of currently
enhanced seismicity around the Inn valley is likely to mostly occur on a single active fault source or strongly interrelated
fault sources linked in connection with activity at the sub-Tauern ramp (Ortner et al., 2006; Reiter et al., 2018). Additionally,
515 constant tectonic loading of these faults is caused by ongoing 1-2 mm/year N-ward pushing of the Adriatic microplate
(Métois et al., 2015) located directly south of the study area.

The paleoseismic catalogue also provides insights in the spatio-temporal patterns of strong earthquake occurrence from the
two inneralpine records Achensee and Piburgersee (Fig. 4a). A high event frequency (590 years recurrence rate) occurred at
~12 to ~8 ka BP at Achensee during which only one event is documented at Piburgersee. In contrast, the period of ~7 to ~3
520 ka BP is characterized by a high event frequency (540 years recurrence rate) at Piburgersee and only two events in Achensee.
Since then, three events are recorded in Achensee but none in Piburgersee. This observation potentially indicates a spatial
shift of paleoseismicity from east to west to east in postglacial times. Strikingly, the proposed periods of enhanced seismicity
at Achensee and Piburgersee both end with an outstanding severe earthquake, as documented by the size and amount of their
sedimentary imprints (Fig. 4a). Whether such a particularly severe earthquake significantly altered the local stress field by
525 releasing a significant portion of energy accumulated by tectonic loading in the respective area, or this observation is just
coincidence cannot be resolved by the available amount of paleoseismic archives.

A maximum credible earthquake magnitude of M_w 6 (+0.5 if a strike slip mechanism was involved) was previously assessed
based on macroseismic data in this region (Lenhardt et al., 2007). The presented paleo-earthquake scenarios provide data-
based observational evidence that an earthquake with a maximum credible magnitude e.g. the M_w 6.0-6.3 at ~8.3 ka BP at
530 Achensee happened several times in the study area during the past 16 kyrs. In particular, this has implications for the seismic
demand in the building code of critical infrastructure such as dam structures, which are constructed based on the assessed
maximum credible earthquake (Zenz and Oberhuber, 2002). In contrast, these findings do not have implications for the
seismic design of general buildings and infrastructure (ÖNORM B 1998-1, 2011), as the recurrence interval of all three
records combined (~630 years) is larger than the therein considered recurrence interval (475 years or 10% probability of
535 exceedance within 50 years). However, it remains to future earthquake hazard assessments and policy makers to find



adequate strategies to implement such low frequency-high impact scenarios, evaluate available mitigation and response strategies in case of such a cross-border event and prepare the society also in intraplate tectonic regions for a possible worst-case scenario.

6 Conclusions

540 The first lacustrine paleoseismic archives of the western Eastern Alps revealed in total 25 sedimentary imprints of severe seismic shaking expressed as multiple, coeval MTDs, SSDS or subaqueous surface ruptures. At the individual studied lake sites, seismic shaking with $SI > VI\frac{1}{4}$ occurs every 1,000-2,000 years in a weakly periodic to aperiodic recurrence behavior. Severe paleo-earthquakes with minimum magnitudes of M_w 5.8-6.1 might have occurred in the present-day zone of enhanced seismicity around the Inn valley, Brenner region and Fernpass region, but also in the present-day low seismicity zone of the upper Loisach region. A surface-rupturing earthquake at Achensee is constrained to M_w 6.0-6.3. NE-SW migration of paleo-earthquakes between circa 6.5 to 3.0 ka BP might hint at a progressive failure along the Fernpass-Loisach fault. Moreover, a shift of paleoseismicity from east to west to east in the area of the Inn valley during Postglacial times might be indicated by the regional paleo-earthquake catalogue. The shakemaps of paleo-earthquake scenarios highlight that severe earthquakes in the study area could strongly affect the northern foreland regions. Complementary paleoseismic investigations especially north and east of the study area are required to evaluate and further improve these initial results.

7 Data availability

Data and codes are available from the authors upon request.

8 Author contribution

555 JM, MS and PO designed the study. PO, JM and MS acquired reflection seismic and core data, calculated earthquake recurrence statistics, generated the paleo-earthquake scenarios and interpreted the results. JS wrote the code of the shakemaps. PO wrote the manuscript and produced the figures with input from all co-authors.

9 Competing interests

560 The authors declare that they have no conflict of interest.



10 Acknowledgments

This research is funded by the Tyrolean Science Fund (TWF): UNI-16588/5-2019, the Austrian Science Fund (FWF): P30285-N34 and European Regional Development Fund Interreg 312 V-A (project ITAT-301 6). We thank Markus Erhardt, Gerald Degenhart and Wolfgang Recheis for the medical CT measurements at the Medical University of Innsbruck and Irka Hajdas for radiocarbon measurements. Land Tirol - data.tirol.gv.at is thanked for providing the DEM data. IHS Markit is acknowledged for their educational grant program providing the Kingdom seismic interpretation software.

11 References

- Avşar, U., Jónsson, S., Avşar, Ö. and Schmidt, S.: Earthquake-induced soft-sediment deformations and seismically amplified erosion rates recorded in varved sediments of Köyceğiz Lake (SW Turkey), *J. Geophys. Res. Solid Earth*, 121(6), 4767–4779, doi:10.1002/2016JB012820, 2016.
- Bakun, W. H. and Wentworth, C. M.: Estimating earthquake location and magnitude from seismic intensity data, *Bulletin Seismol. Soc. Am.*, 87(6), 1502–1521, 1997.
- Beck, C.: Late Quaternary lacustrine paleo-seismic archives in north-western Alps: Examples of earthquake-origin assessment of sedimentary disturbances”, *Earth-Science Rev.*, 96(4), 327–344, doi:10.1016/j.earscirev.2009.07.005, 2009.
- Beck, C., Manalt, F., Chapron, E., Rensbergen, P. Van and Batist, M. De: Enhanced seismicity in the early post-glacial period: Evidence from the post-würm sediments of lake annecy, northwestern Alps, *J. Geodyn.*, 22(1–2), 155–171, doi:10.1016/0264-3707(96)00001-4, 1996.
- Bellwald, B.: Paleoseismologic Implication Sof the Sediment Stratigraphy in Lake Silvaplana (Engadine, Eastern Switzerland), Master Thesis, ETH Zürich, Zürich., 2012.
- Bellwald, B., Hjelstuen, B. O., Sejrup, H. P., Stokowy, T. and Kuvås, J.: Holocene mass movements in west and mid-Norwegian fjords and lakes, *Mar. Geol.*, 407(August 2018), 192–212, doi:10.1016/j.margeo.2018.11.007, 2019.
- Blaauw, M. and Christen, J. A.: Flexible paleoclimate age-depth models using an autoregressive gamma process, *Bayesian Anal.*, 6(3), 457–474, doi:10.1214/11-BA618, 2011.
- Brooks, G. R.: Deglacial record of palaeoearthquakes interpreted from mass transport deposits at three lakes near Rouyn-Noranda, north-western Quebec, Canada, edited by N. Eyles, *Sedimentology*, 65(7), 2439–2467, doi:10.1111/sed.12473, 2018.
- Brooks, G. R. and Adams, J.: A review of evidence of glacially-induced faulting and seismic shaking in eastern Canada, *Quat. Sci. Rev.*, 228, 106070, doi:10.1016/j.quascirev.2019.106070, 2020.
- Carulli, G. B. and Slejko, D.: The 1976 Friuli, Italy, Earthquake, *G. di Geol. Appl.*, 1, 147–156, doi:10.1474/GGA.2005-01.0-15.0015, 2005.
- Chassiot, L., Chapron, E., Di Giovanni, C., Albéric, P., Lajeunesse, P., Lehours, A.-C. C. and Meybeck, M.: Extreme events in the sedimentary record of maar Lake Pavin: Implications for natural hazards assessment in the French Massif Central,



- Quat. Sci. Rev., 141, 9–25, doi:10.1016/j.quascirev.2016.03.020, 2016.
- 595 Czymzik, M., Brauer, A., Dulski, P., Plessen, B., Naumann, R., von Grafenstein, U. and Scheffler, R.: Orbital and solar forcing of shifts in Mid- to Late Holocene flood intensity from varved sediments of pre-alpine Lake Ammersee (southern Germany), Quat. Sci. Rev., 61, 96–110, doi:10.1016/j.quascirev.2012.11.010, 2013.
- 600 Van Daele, M., Moernaut, J., Doom, L., Boes, E., Fontijn, K., Heirman, K., Vandoorne, W., Hebbeln, D., Pino, M., Urrutia, R., Brümmer, R. and De Batist, M.: A comparison of the sedimentary records of the 1960 and 2010 great Chilean earthquakes in 17 lakes: Implications for quantitative lacustrine palaeoseismology, Sedimentology, 62(5), 1466–1496, doi:10.1111/sed.12193, 2015.
- Van Daele, M., Haeussler, P. J., Witter, R. C., Praet, N. and De Batist, M.: The sedimentary record of the 2018 Anchorage earthquake in Eklutna Lake, Alaska: Calibrating the lacustrine seismograph, Seismol. Res. Lett., 91(1), 126–141, doi:10.1785/0220190204, 2019.
- 605 Daut, G.: Subaquatische Massenbewegungen im Starnberger See und im Tegernsee, Münchner Geol. Hefte R. B Angew. Geol., B5, 121, 1998.
- Doughty, M., Eyles, N., Eyles, C. H., Wallace, K. and Boyce, J. I.: Lake sediments as natural seismographs: Earthquake-related deformations (seismites) in central Canadian lakes, Sediment. Geol., 313, 45–67, doi:10.1016/j.sedgeo.2014.09.001, 2014.
- 610 Eisbacher, G. H. and Brandner, R.: Superposed fold-thrust structures and high-angle faults, Northwestern Calcareous Alps, Austria, Eclogae Geol. Helv., 89(1), 553–571, 1996.
- Fabbri, S. C., Herwegh, M., Horstmeyer, H., Hilbe, M., Hübscher, C., Merz, K., Schlunegger, F., Schmelzbach, C., Weiss, B. and Anselmetti, F. S.: Combining amphibious geomorphology with subsurface geophysical and geological data: A neotectonic study at the front of the Alps (Bernese Alps, Switzerland), Quat. Int., 451, 101–113, doi:10.1016/j.quaint.2017.01.033, 2017.
- 615 Fabbri, S. C., Affentranger, C., Krastel, S., Lindhorst, K., Wessels, M., Madritsch, H., Allenbach, R., Herwegh, M., Heuberger, S., Wielandt-Schuster, U., Pomella, H., Schwestermann, T. and Anselmetti, F. S.: Active Faulting in Lake Constance (Austria, Germany, Switzerland) Unraveled by Multi-Vintage Reflection Seismic Data, Front. Earth Sci., 9(August), 1–26, doi:10.3389/feart.2021.670532, 2021.
- 620 Fähr, D., Giardini, D., Kästli, P., Deichmann, N., Gisler, M., Schwarz-Zanetti, G., Alvarez-Rubio, S., Sellami, S., Edwards, B., Allmann, B., Behtmann, F., Wössner, J., Gassner-Stamm, G. Fritsche, S. and Eberhard, D.: ECOS-09 Earthquake Catalogue of Switzerland Release 2011. Report and Data., Public catalogue, 17.04.2011., Swiss Seismol. Serv. ETH Zurich, Zurich, 2011.
- Galadini, F. and Galli, P.: Palaeoseismology related to the displaced Roman archaeological remains at Eгна (Adige Valley, northern Italy), Tectonophysics, 308(1–2), 171–191, doi:10.1016/S0040-1951(99)00080-3, 1999.
- 625 Gasperini, L., Marzocchi, A., Mazza, S., Miele, R., Meli, M., Najjar, H., Michetti, A. M. and Polonia, A.: Morphotectonics and late Quaternary seismic stratigraphy of Lake Garda (Northern Italy), Geomorphology, 371, 107427,



- doi:10.1016/j.geomorph.2020.107427, 2020.
- Goh, K.-I. and Barabási, A.-L.: Burstiness and memory in complex systems, *EPL (Europhysics Lett.)*, 81(4), 48002, doi:10.1209/0295-5075/81/48002, 2008.
- 630 Griffin, J. D., Stirling, M. W. and Wang, T.: Periodicity and Clustering in the Long-Term Earthquake Record, *Geophys. Res. Lett.*, 47(22), doi:10.1029/2020GL089272, 2020.
- Grünthal, G.: European Macroseismic Scale 1998 EMS-98, *Eur. Seismol. Comm. Subcomm. Eng. Seismol. Work. Gr. Macroseismic Scales. Cons. l'Europe, Cah. du Cent. Eur. Géodynamique Séismologie*, 99, 1998.
- Hammerl, C.: Historical earthquake research in Austria, *Geosci. Lett.*, 4(1), 99, doi:10.1186/s40562-017-0073-8, 2017.
- 635 Hammerl, C., Lenhardt, W. A. and Innerkofler, M.: Forschungen zu den stärksten historischen Erdbeben im mittleren Inntal im Rahmen des INTERREG IV-Projekts HAREIA (Historical And Recent Earthquakes in Italy and Austria), *Forum Hall Tirol. Neues zur Geschichte der Stadt*, 3, 2012.
- Howarth, J. D., Fitzsimons, S. J., Norris, R. J. and Jacobsen, G. E.: Lake sediments record high intensity shaking that provides insight into the location and rupture length of large earthquakes on the Alpine Fault, New Zealand, *Earth Planet. Sci. Lett.*, 403, 340–351, doi:10.1016/j.epsl.2014.07.008, 2014.
- 640 Howarth, J. D., Fitzsimons, S. J., Norris, R. J., Langridge, R. and Vandergoes, M. J.: A 2000 yr rupture history for the Alpine fault derived from Lake Ellery, South Island, New Zealand, *Bull. Geol. Soc. Am.*, 128(3–4), 627–643, doi:10.1130/B31300.1, 2016.
- Ivy-Ochs, S., Kerschner, H., Reuther, A., Preusser, F., Heine, K., Maisch, M., Kubik, P. W. and Schlüchter, C.: Chronology of the last glacial cycle in the European Alps, *J. Quat. Sci.*, 23(6–7)(4), 559–573, 2008.
- 645 Kempf, P. and Moernaut, J.: Age Uncertainty in Recurrence Analysis of Paleoseismic Records, *Manuscr. Submitt. to J. Geophys. Res. Solid Earth*, 29, doi:<https://doi.org/10.1002/essoar.10506437.3>, 2021.
- Kiefer, C., Oswald, P., Moernaut, J., Fabbri, S. C., Mayr, C., Strasser, M. and Krautblatter, M.: A 4 ka debris flow record based on amphibious investigations of fan delta activity in Plansee (Austria, Eastern Alps), *Earth Surf. Dyn.*, 2021.
- 650 Kremer, K., Wirth, S. B., Reusch, A., Fäh, D., Bellwald, B., Anselmetti, F. S., Girardclos, S. and Strasser, M.: Lake-sediment based paleoseismology: Limitations and perspectives from the Swiss Alps, *Quat. Sci. Rev.*, 168, 1–18, doi:10.1016/j.quascirev.2017.04.026, 2017.
- de La Taille, C., Jouanne, F., Crouzet, C., Beck, C., Jomard, H., de Rycker, K. and van Daele, M.: Impact of active faulting on the post LGM infill of Le Bourget Lake (western Alps, France), *Tectonophysics*, 664, 31–49, doi:10.1016/j.tecto.2015.08.024, 2015.
- 655 Lauterbach, S., Chapron, E., Brauer, A., Hüls, M., Gilli, A., Arnaud, F., Piccin, A., Nomade, J., Desmet, M., von Grafenstein, U. and Participants, D.: A sedimentary record of Holocene surface runoff events and earthquake activity from Lake Iseo (Southern Alps, Italy), *The Holocene*, 22(7), 749–760, doi:10.1177/0959683611430340, 2012.
- Lemaire, E., Mreyen, A.-S., Dufresne, A. and Havenith, H.-B.: Analysis of the Influence of Structural Geology on the Massive Seismic Slope Failure Potential Supported by Numerical Modelling, *Geosciences*, 10(8), 323,
- 660



- doi:10.3390/geosciences10080323, 2020.
- Lenhardt, W. A., Freudenthaler, C., Lippitsch, R. and Fiegweil, E.: Focal-depth distributions in the Austrian Eastern Alps based on macroseismic data, *Austrian J. Earth Sci.*, 100, 66–79, 2007.
- Liu, M., Stein, S. and Wang, H.: 2000 years of migrating earthquakes in North China: How earthquakes in midcontinents differ from those at plate boundaries, *Lithosphere*, 3(2), 128–132, doi:10.1130/L129.1, 2011.
- 665 Mancktelow, N., Zwingmann, H., Campani, M., Fügenschuh, B. and Mulch, A.: Timing and conditions of brittle faulting on the Silltal-Brenner Fault Zone, Eastern Alps (Austria), *Swiss J. Geosci.*, 108(2–3), 305–326, doi:10.1007/s00015-015-0179-y, 2015.
- Mazzotti, S., Jomard, H. and Masson, F.: Processes and deformation rates generating seismicity in metropolitan France and conterminous Western Europe, *BSGF - Earth Sci. Bull.*, 191, 0–20, doi:10.1051/bsgf/2020019, 2020.
- 670 Métois, M., D’Agostino, N., Avallone, A., Chamot-Rooke, N., Rabaute, A., Duni, L., Kuka, N., Koci, R. and Georgiev, I.: Insights on continental collisional processes from GPS data: Dynamics of the peri-Adriatic belts, *J. Geophys. Res. Solid Earth*, 120(12), 8701–8719, doi:10.1002/2015JB012023, 2015.
- Moernaut, J.: Time-dependent recurrence of strong earthquake shaking near plate boundaries: A lake sediment perspective, *Earth-Science Rev.*, 210(August), 103344, doi:10.1016/j.earscirev.2020.103344, 2020.
- 675 Moernaut, J., van Daele, M., Heirman, K., Fontijn, K., Strasser, M., Pino, M., Urrutia, R. and de Batist, M.: Lacustrine turbidites as a tool for quantitative earthquake reconstruction: New evidence for a variable rupture mode in south central Chile, *J. Geophys. Res. Solid Earth*, 119(3), 1607–1633, doi:10.1002/2013JB010738, 2014.
- Molenaar, A., Van Daele, M., Vandorpe, T., Degenhart, G., De Batist, M., Urrutia, R., Pino, M., Strasser, M. and Moernaut, J.: What controls the remobilization and deformation of surficial sediment by seismic shaking? Linking lacustrine slope stratigraphy to great earthquakes in South–Central Chile, *Sedimentology*, doi:10.1111/sed.12856, 2021.
- 680 Monecke, K., Anselmetti, F. S., Becker, A., Sturm, M. and Giardini, D.: The record of historic earthquakes in lake sediments of Central Switzerland, *Tectonophysics*, 394(1–2), 21–40, doi:10.1016/j.tecto.2004.07.053, 2004.
- ÖNORM B 1998-1: Eurocode 8: Auslegung von Bauwerken gegen Erdbeben. Teil 1: Grundlagen, Erdbebeneinwirkungen und Regeln für Hochbauten. Ausgabe 201106-15. Ersatz für ÖNORM EN 1998-1:2005-06, Austrian Standards Institute (ON), 2011.
- 685 Ortner, H., Reiter, F. and Brandner, R.: Kinematics of the Inntal shear zone-sub-Tauern ramp fault system and the interpretation of the TRANSALP seismic section, Eastern Alps, Austria, *Tectonophysics*, 414(1–4), 241–258, doi:10.1016/j.tecto.2005.10.017, 2006.
- 690 Oswald, P., Moernaut, J., Fabbri, S. C., De Batist, M., Hajdas, I., Ortner, H., Titzler, S. and Strasser, M.: Combined On-Fault and Off-Fault Paleoseismic Evidence in the Postglacial Infill of the Inner-Alpine Lake Achensee (Austria, Eastern Alps), *Front. Earth Sci.*, 9, 438, doi:10.3389/feart.2021.670952, 2021a.
- Oswald, P., Strasser, M., Hammerl, C. and Moernaut, J.: Seismic control of large prehistoric rockslides in the Eastern Alps, *Nat. Commun.*, doi:10.1038/s41467-021-21327-9, 2021b.



- 695 Petersen, J., Wilhelm, B., Revel, M., Rolland, Y., Crouzet, C., Arnaud, F., Brisset, E., Chaumillon, E. and Magand, O.: Sediments of Lake Vens (SW European Alps, France) record large-magnitude earthquake events, *J. Paleolimnol.*, 51(3), 343–355, doi:10.1007/s10933-013-9759-x, 2014.
- Plan, L., Grasemann, B., Spötl, C., Decker, K., Boch, R. and Kramers, J.: Neotectonic extrusion of the Eastern Alps: Constraints from U/Th dating of tectonically damaged speleothems, *Geology*, 38(6), 483–486, 2010.
- 700 Praet, N., Moernaut, J., van Daele, M., Boes, E., Haeussler, P. J., Strupler, M., Schmidt, S., Loso, M. G. and de Batist, M.: Paleoseismic potential of sublacustrine landslide records in a high-seismicity setting (south-central Alaska), *Mar. Geol.*, 384, 103–119, doi:10.1016/j.margeo.2016.05.004, 2017.
- Praet, N., Van Daele, M., Collart, T., Moernaut, J., Vandekerckhove, E., Kempf, P., Haeussler, P. J. and De Batist, M.: Turbidite stratigraphy in proglacial lakes: Deciphering trigger mechanisms using a statistical approach, edited by F. Felletti, *Sedimentology*, 67(5), 2332–2359, doi:10.1111/sed.12703, 2020.
- 705 Prager, C., Zangerl, C., Patzelt, G. and Brandner, R.: Age distribution of fossil landslides in the Tyrol (Austria) and its surrounding areas, *Nat. Hazards Earth Syst. Sci.*, 8(2), 377–407, doi:10.5194/nhess-8-377-2008, 2008.
- Ratschbacher, L., Merle, O., Davy, P. and Cobbold, P.: Lateral extrusion in the eastern Alps, Part 1: Boundary conditions and experiments scaled for gravity, *Tectonics*, 10(2), 245–256, doi:10.1029/90TC02622, 1991.
- 710 Reiter, F., Freudenthaler, C., Hausmann, H., Ortner, H., Lenhardt, W. and Brandner, R.: Active Seismotectonic Deformation in Front of the Dolomites Indenter, Eastern Alps, *Tectonics*, 37(12), 4625–4654, doi:10.1029/2017TC004867, 2018.
- Rosenberg, C. L., Brun, J. P. and Gapais, D.: Indentation model of the Eastern Alps and the origin of the Tauern Window, *Geology*, 32(11), 997–1000, doi:10.1130/G20793.1, 2004.
- Rudloff, A. and Leydecker, G.: Ableitung von empirischen Beziehungen zwischen der Lokalbebenmagnitude und makroseismischen Parametern-Ergebnisbericht, BGR, Hann., 45 [online] Available from: https://scholar.google.at/scholar?hl=en&as_sdt=0%2C5&q=Rudloff+and+Leydecker+%282002%29+&btnG= (Accessed 4 August 2021), 2002.
- Schwestermann, T.: Mass-movement event stratigraphy in lake constance, Master thesis, ETH Zürich, Zürich., 2016.
- Serva, L., Vittori, E., Comerci, V., Esposito, E., Guerrieri, L., Michetti, A. M., Mohammadioun, B., Mohammadioun, G. C.,
- 720 Porfido, S. and Tatevossian, R. E.: Earthquake Hazard and the Environmental Seismic Intensity (ESI) Scale, *Pure Appl. Geophys.*, 173(5), 1479–1515, doi:10.1007/s00024-015-1177-8, 2016.
- Simonneau, A., Chapron, E., Vannière, B., Wirth, S. B., Gilli, A., Di Giovanni, C., Anselmetti, F. S., Desmet, M. and Magny, M.: Mass-movement and flood-induced deposits in Lake Ledro, southern Alps, Italy: Implications for Holocene palaeohydrology and natural hazards, *Clim. Past*, 9(2), 825–840, doi:10.5194/cp-9-825-2013, 2013.
- 725 Slejko, D.: What science remains of the 1976 Friuli earthquake?, *Boll. di Geofis. Teor. ed Appl.*, 59(4), 327–350, doi:10.4430/bgta0224, 2018.
- Sponheuer, W.: Methoden zur Herdtiefenbestimmung in der Makroseismik, Akademie-Verlag, Berlin. [online] Available from:



- 730 https://scholar.google.at/scholar?hl=en&as_sdt=0%2C5&q=Sponheuer%2C+W.+%281960%29+Methoden+zur+Herdiefen+bestimmung+in+der+Makroseismik.+Freiberger+Forschungs-Hefte%2C+C88%2C+120+S.&btnG= (Accessed 4 August 2021), 1960.
- Stein, R. S., Barka, A. A. and Dieterich, J. H.: Progressive failure on the North Anatolian fault since 1939 by earthquake stress triggering, *Geophys. J. Int.*, 128, 594–604, 1997.
- Stirling, M., Rhoades, D. and Berryman, K.: Comparison of Earthquake Scaling Relations Derived from Data of the
735 Instrumental and Preinstrumental Era, *Bull. Seismol. Soc. Am.*, 92(2), 812–830, doi:10.1785/0120000221, 2002.
- Strasser, M. and Anselmetti, F.: Mass-movement event stratigraphy in Lake Zurich; a record of varying seismic and environmental impacts, *Beitr`Ige zur Geol. Schw., Geotechn. Ser.*, 95, 23–41 [online] Available from: <http://scholar.google.com/scholar?hl=en&btnG=Search&q=intitle:MASS-MOVEMENT+EVENT+STRATIGRAPHY+IN+LAKE+ZURICH:+A+RECORD+OF+VARYING+SEISMIC+AND+ENVIRONMENTAL+IMPACTS#0>,
740 IRONMENTAL+IMPACTS#0, 2008.
- Strasser, M., Anselmetti, F. S., Fäh, D., Giardini, D. and Schnellmann, M.: Magnitudes and source areas of large prehistoric northern Alpine earthquakes revealed by slope failures in lakes, *Geology*, 34(12), 1005, doi:10.1130/G22784A.1, 2006.
- Strasser, M., Monecke, K., Schnellmann, M. and Anselmetti, F. S.: Lake sediments as natural seismographs: A compiled record of Late Quaternary earthquakes in Central Switzerland and its implication for Alpine deformation, *Sedimentology*,
745 60(1), 319–341, doi:10.1111/sed.12003, 2013.
- Stucchi, M., Rovida, A., Gomez Capera, A. A., Alexandre, P., Camelbeeck, T., Demircioglu, M. B., Gasperini, P., Kouskouna, V., Musson, R. M. W., Radulian, M., Sesetyan, K., Vilanova, S., Baumont, D., Bungum, H., Fäh, D., Lenhardt, W., Makropoulos, K., Martinez Solares, J. M., Scotti, O., Živčić, M., Albini, P., Batllo, J., Papaioannou, C., Tatevossian, R., Locati, M., Meletti, C., Viganò, D. and Giardini, D.: The SHARE European Earthquake Catalogue (SHEEC) 1000-1899, *J.*
750 *Seismol.*, 17(2), 523–544, doi:10.1007/s10950-012-9335-2, 2013.
- Ustaszewski, M. and Pfiffner, O. a.: Neotectonic faulting, uplift and seismicity in the central and western Swiss Alps, *Geol. Soc. London, Spec. Publ.*, 298(1), 231–249, doi:10.1144/SP298.12, 2008.
- Vanneste, K., Wils, K. and Van Daele, M.: Probabilistic Evaluation of Fault Sources Based on Paleoseismic Evidence From Mass-Transport Deposits: The Example of Aysén Fjord, Chile, *J. Geophys. Res. Solid Earth*, doi:10.1029/2018JB016289,
755 2018.
- Vasskog, K., Nesje, A., Støren, E. N., Waldmann, N., Chapron, E. and Ariztegui, D.: A Holocene record of snow-avalanche and flood activity reconstructed from a lacustrine sedimentary sequence in Oldevatnet, western Norway, *The Holocene*, 21(4), 597–614, doi:10.1177/0959683610391316, 2011.
- Wetzler, N., Marco, S. and Heifetz, E.: Quantitative analysis of seismogenic shear-induced turbulence in lake sediments,
760 *Geology*, 38(4), 303–306, doi:10.1130/G30685.1, 2010.
- Wilhelm, B., Nomade, J., Crouzet, C., Litty, C., Sabatier, P., Belle, S., Rolland, Y., Revel, M., Courboulex, F., Arnaud, F. and Anselmetti, F. S.: Quantified sensitivity of small lake sediments to record historic earthquakes: Implications for



- paleoseismology, *J. Geophys. Res. Earth Surf.*, 121(1), 2–16, doi:10.1002/2015JF003644, 2016.
- Williams, R. T., Davis, J. R. and Goodwin, L. B.: Do Large Earthquakes Occur at Regular Intervals Through Time? A
765 Perspective From the Geologic Record, *Geophys. Res. Lett.*, 46(14), 8074–8081, doi:10.1029/2019GL083291, 2019.
- Wils, K., Deprez, M., Kissel, C., Vervoort, M., Van Daele, M., Daryono, M. R., Cnudde, V., Natawidjaja, D. H. and De
Batist, M.: Earthquake doublet revealed by multiple pulses in lacustrine seismo-turbidites, *Geology*, doi:10.1130/G48940.1,
2021.
- Zenz, G. and Oberhuber, P.: Erdbebenberechnung von Talsperren in Österreich, *Wasserwirtschaft*, 92(10), 2–8, 2002.
- 770 Zimmermann, J.: Der Walensee - eine sedimentologische Rekonstruktion seiner holozänen Ereignisgeschichte, Master
Thesis, EAWAG, Zürich., 2008.